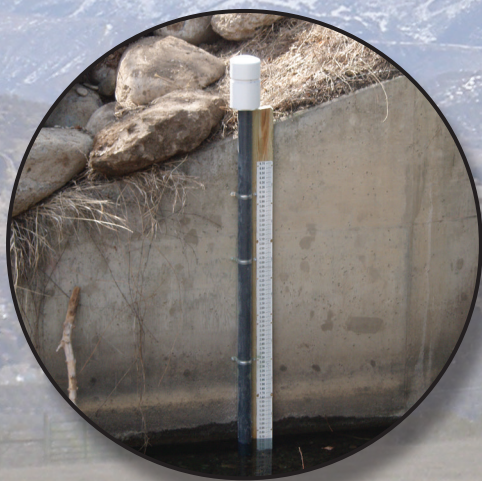


Prepared in cooperation with the Bureau of Reclamation and the Colorado River Salinity Control Forum

Characterization of Salinity Loads and Selenium Loads in the Smith Fork Creek Region of the Lower Gunnison River Basin, Western Colorado, 2008–2009



Scientific Investigations Report 2014–5101

Cover. *Upper center (and background),* West Elk Mountains with Needle Rock in foreground, near Crawford, Colorado, February 2009. Photograph by Josh Linard, U.S. Geological Survey.

Lower left, Gage installation at site SF2, 2008. Photograph by Robert Wilson, formerly with the U.S. Geological Survey.

Lower right, Canyon Ranch, looking southeast, November 2009. Photograph by Rodney Richards, U.S. Geological Survey.

Characterization of Salinity Loads and Selenium Loads in the Smith Fork Creek Region of the Lower Gunnison River Basin, Western Colorado, 2008–2009

By Rodney J. Richards, Joshua I. Linard, and Christopher M. Hobza

Prepared in cooperation with the Bureau of Reclamation and the Colorado River Salinity Control Forum

Scientific Investigations Report 2014–5101

U.S. Department of the Interior
U.S. Geological Survey

U.S. Department of the Interior

SALLY JEWELL, Secretary

U.S. Geological Survey

Suzette M. Kimball, Acting Director

U.S. Geological Survey, Reston, Virginia: 2014

For more information on the USGS—the Federal source for science about the Earth, its natural and living resources, natural hazards, and the environment, visit <http://www.usgs.gov> or call 1–888–ASK–USGS.

For an overview of USGS information products, including maps, imagery, and publications, visit <http://www.usgs.gov/pubprod>

To order this and other USGS information products, visit <http://store.usgs.gov>

Any use of trade, firm, or product names is for descriptive purposes only and does not imply endorsement by the U.S. Government.

Although this information product, for the most part, is in the public domain, it also may contain copyrighted materials as noted in the text. Permission to reproduce copyrighted items must be secured from the copyright owner.

Suggested citation:

Richards, R.J., Linard, J.I., and Hobza, C.M., 2014, Characterization of salinity loads and selenium loads in the Smith Fork Creek region of the Lower Gunnison River Basin, western Colorado, 2008–2009: U.S. Geological Survey Scientific Investigations Report 2014–5101, 34 p., <http://dx.doi.org/10.3133/sir20145101>.

ISSN 2328-0328 (online)

Contents

Abstract.....	1
Introduction.....	1
Purpose and Scope	2
Description of Study Area	2
Climate and Hydrology	4
Geology.....	4
Data Collection and Analysis	4
Sampling and Data Analysis	5
Water Budget	5
Salinity Budget.....	7
Off-Farm Salinity Load Estimation	8
VS2DH Model Framework, Data Collection, and Calibration	8
Data Collection—Mancos Shale Site Model	10
Model Framework—Mancos Shale Site	10
Model Calibration—Mancos Shale Site (Km).....	12
Data Collection—Dakota Sandstone and Burro Canyon Formation Site Model.....	13
Model Framework—Dakota Sandstone and Burro Canyon Formation Site	14
Model Calibration—Dakota Sandstone and Burro Canyon Formation (Kdb).....	14
Salinity Loads from Agricultural Land	15
Tail-Water Salinity Loads.....	15
Deep Percolation Salinity Loads	15
Natural Salinity Load Estimation	16
Nonagricultural Salinity Load Estimation	16
Selenium Load Estimation	17
Error Analysis	17
Salinity Load Error Analysis	18
Selenium Load Error Analysis.....	18
Characterization of Salinity Loads and Selenium Loads.....	19
Water Budget	19
Salinity Loads.....	20
Natural Salinity Load	20
Agricultural Salinity Load	21
Total Salinity Load	21
Percent of Agricultural Salinity Load within the Total Salinity Load	23
Selenium Loads	24
Summary.....	26
Acknowledgments.....	27
References.....	28
Appendixes	31
1. Lithological Descriptions of Sediment Cores Collected from Various Drilled Well Holes at Sites Km and Kdb.....	33
2. Measured Canal Temperature and Specific Conductance Data in the Study Area	34

Figures

1. Location of study area and subbasins, water-quality sites, irrigated land, and water delivery canals within the study area	3
2. Location of heat-tracer investigations sites in relation to the study area	9
3. Generalized installation diagram for site Km	11
4. Generalized one-dimensional VS2DH model for site Km	11
5. Observed temperature, gage height, pressure head, and hydraulic gradient at site Km	12
6. Observed and simulated subsurface temperature data at various depths below the canal bottom at site Km	13
7. Generalized installation diagram for site Kdb	14
8. Generalized two-dimensional VS2DH model for site Kdb	15
9. Observed temperature, canal stage, and water level data for site Kdb	16
10. Calculated daily seepage rate, using the boundary flux extension of VS2DH at site Km	20
11. Calculated daily seepage rate, using the boundary flux extension of VS2DH at site Kdb	20
12. Total salinity load, with error bars	23
13. Location of ungaged portion of Alum Gulch in relation to site AL1	24
14. Relative magnitude of total salinity loads and the proportion of on-farm, off-farm, and natural salinity load for each subbasin in the study area	25
15. Surface water selenium loads, with error bars	26

Tables

1. U.S. Geological Survey water-quality data collection sites in the study area, April 2008–March 2009	5
2. Summary of gage height to streamflow ratings at selected sites in the study area, April 2008–March 2009	7
3. Summary of equations for estimating total dissolved solids for specific conductance in agricultural and natural subbasin types	7
4. Calculated average base-flow concentrations of total dissolved solids for selected subbasins in the study area, April 2008–March 2009	8
5. Calibrated VS2DH model parameters for simulation of hydraulic conductivity at heat-tracer test sites	10
6. Ratios used to separate canal seepage and deep percolation from drain base flow	17
7. Summary of ratios of surface-water selenium concentration to salinity concentration at selected sites in the study area	17
8. Summary of water budget allocations at selected sites in the study area, April 2008–March 2009	19
9. Summary of seepage rates calculated using the boundary flux extension of the VS2DH model at sites Km and Kdb	20
10. Summary of annual agricultural salinity loads at selected sites in the study area, April 2008–March 2009	21
11. Estimated monthly gaged-salinity loads at selected sites in the study area, April 2008–March 2009	21

12.	Summary of annual salinity loads at selected sites in the study area, April 2008–March 2009.....	22
13.	Summary of associated error in the annual salinity load estimations in the study area, April 2008–March 2009.....	23
14.	Salinity yield and subbasin land use area used to calculate the total salinity load at the confluence of Alum Gulch and the North Fork of the Gunnison River.....	25
15.	Summary of gaged selenium loads at selected sites in the study area, April 2008–March 2009.....	26

Conversion Factors

Inch/Pound to SI

Multiply	By	To obtain
Length		
inch (in.)	25.4	millimeter (mm)
inch (in.)	2.54	centimeter (cm)
foot (ft)	0.3048	meter (m)
mile (mi)	1.609	kilometer (km)
Area		
acre	0.004047	square kilometer (km ²)
Volume		
cubic foot (ft ³)	0.02832	cubic meter (m ³)
acre-foot (acre-ft)	1,233	cubic meter (m ³)
Flow rate		
acre-foot per day (acre-ft/d)	0.01427	cubic meter per second (m ³ /s)
acre-foot per year (acre-ft/yr)	1,233	cubic meter per year (m ³ /yr)
cubic foot per second (ft ³ /s)	0.02832	cubic meter per second (m ³ /s)
Yield		
tons per acre	0.9072	metric tons per acre
Mass		
pound, avoirdupois (lb)	0.4536	kilogram (kg)
ton, short (2,000 lb)	0.9072	megagram (Mg)
Pounds per day (lb/d)	0.454	kilograms per day (k/d)
ton per year (ton/yr)	0.9072	metric ton per year
Hydraulic conductivity		
foot per day (ft/d)	0.3048	meter per day (m/d)
Energy		
joule (J)	0.00027	watt-hour (Wh)

Temperature in degrees Celsius (°C) may be converted to degrees Fahrenheit (°F) as follows:

$$^{\circ}\text{F} = (1.8 \times ^{\circ}\text{C}) + 32$$

Temperature in degrees Fahrenheit (°F) may be converted to degrees Celsius (°C) as follows:

$$^{\circ}\text{C} = (^{\circ}\text{F} - 32)/1.8$$

Vertical coordinate information is referenced to the North American Vertical Datum of 1988 (NAVD 88).

Horizontal coordinate information is referenced to the North American Datum of 1983 (NAD 83).

Specific conductance is given in microsiemens per centimeter at 25 degrees Celsius (μS/cm at 25 °C).

Water year, A water year is the 12-month period from October 1 for any given year through September 30 of the following year. The water year is designated by the calendar year in which it ends and which includes 9 of the 12 months. Thus, the year ending September 30, 2008, is called the “2008” water year.

Characterization of Salinity Loads and Selenium Loads in the Smith Fork Creek Region of the Lower Gunnison River Basin, Western Colorado, 2008–2009

By Rodney J. Richards, Joshua I. Linard, and Christopher M. Hobza

Abstract

The lower Gunnison River Basin of the Colorado River Basin has elevated salinity and selenium levels. The Colorado River Basin Salinity Control Act of June 24, 1974 (Public Law 93–320, amended by Public Law 98–569), authorized investigation of the Lower Gunnison Basin Unit Salinity Control Project by the U.S. Department of the Interior. The Bureau of Reclamation (Reclamation) and the Natural Resources Conservation Service are responsible for assessing and implementing measures to reduce salinity and selenium loading in the Colorado River Basin. Cost-sharing programs help farmers, ranchers, and canal companies improve the efficiency of water delivery systems and irrigation practices. The delivery systems (irrigation canals) have been identified as potential sources of seepage, which can contribute to salinity loading. Reclamation wants to identify seepage from irrigation systems in order to maximize the effectiveness of the various salinity-control methods, such as polyacrylamide lining and piping of irrigation canals programs. The U.S. Geological Survey, in cooperation with Reclamation, developed a study to characterize the salinity and selenium loading of seven subbasins in the Smith Fork Creek region and identify where control efforts can be maximized to reduce salinity and selenium loading.

Total salinity loads ranged from 27.9 ± 19.1 tons per year (t/yr) to $87,500 \pm 80,500$ t/yr. The four natural subbasins—BkKm, RCG1, RCG2, and SF1—had total salinity loads of 27.9 ± 19.1 t/yr, 371 ± 248 t/yr, $2,180 \pm 1,590$ t/yr, and $4,200 \pm 2,720$ t/yr, respectively. The agriculturally influenced sites had salinity loads that ranged from $7,580 \pm 6,900$ t/yr to $87,500 \pm 80,500$ t/yr. Salinity loads for the subbasins AL1, B1, CK1, SF2, and SF3 were $7,580 \pm 6,900$ t/yr; $28,300 \pm 26,700$ t/yr; $48,700 \pm 36,100$ t/yr; $87,500 \pm 80,900$ t/yr; and $52,200 \pm 31,800$ t/yr, respectively.

The agricultural salinity load was separated into three components: tail water, deep percolation, and canal seepage. Annual tail-water salinity loads ranged from 48.0 to 2,750 tons in the Smith Fork Creek region. The largest tail-water salinity load was in subbasin SF3, and the lowest salinity load from tail water was in subbasin R1. The remaining four agricultural

subbasins—AL1, B1, CK1, and SF2—had tail-water loads of 285 t/yr, 180 t/yr, 333 t/yr, and 1,700 t/yr, respectively.

The deep percolation component of the agricultural salinity load ranged from 3,300 t/yr in subbasin AL1 to 51,800 t/yr in subbasin SF2. Subbasins R1, B1, CK1, and SF3 had deep percolation salinity loads of 4,940 t/yr, 15,200 t/yr, 21,200 t/yr, and 23,600 t/yr, respectively. The canal seepage component of the agricultural salinity load ranged from 1,100 t/yr in subbasin AL1 to 15,300 t/yr in subbasin CK1. Subbasins B1, R1, SF2, and SF3 had canal seepage salinity loads of 6,610 t/yr, 3,890 t/yr, 9,430 t/yr, and 12,100 t/yr, respectively.

Four natural subbasins—RCG1, RCG2, SF1, and BkKm—were used to calculate natural salinity yields for the remaining subbasins. The appropriate salinity yield was applied to the corresponding number of acres and resulted in a natural salinity load for each subbasin. The annual salinity yields for the Dakota Sandstone and Burro Canyon Formation, Mancos Shale, and crystalline geologies are 0.217 tons per acre (t/acre), 0.113 t/acre, and 0.151 t/acre, respectively.

Three of the four natural subbasins had little to no selenium load based on the measured data and calculated selenium loads. Subbasins RCG1 and RCG2 had surface-water selenium loads of 0.106 ± 0.024 pounds (lb) and 0.00 lb, respectively. Subbasin BkKm did not have an estimated surface-water selenium load because of the lack of any water-quality samples during the study period. The subbasin designated by site CK1 had the highest selenium load with 135 ± 38.7 lb, and the next highest subbasins in decreasing order are B1, SF3, AL1, SF1, and R1 with selenium loads of 69.6 ± 28.4 lb, 56.5 ± 23.8 lb, 30.5 ± 16.6 lb, 26.8 ± 6.95 lb, and 15.6 ± 27.7 lb, respectively.

Introduction

The lower Gunnison River Basin of the Colorado River Basin has elevated salinity and selenium (Se) levels (Butler and Leib, 2002; Mayo and Leib, 2012). The Colorado River Basin Salinity Control Act of June 24, 1974 (Public Law 93–320, amended by Public Law 98–569), authorized investigation of the Lower Gunnison Basin Unit Salinity Control

Project by the U.S. Department of the Interior. Salinity is generally defined as the concentration of dissolved mineral salts or dissolved solids in water. Elevated salinity concentrations can cause soil dispersion and corrosion of infrastructure for potable water supplies and irrigation delivery systems. Selenium is a trace metal that bioaccumulates in aquatic food chains and has the potential to cause deformities and reproductive failure in birds and fish, including endangered fish species (Lemly, 2002). Previous studies conducted by the U.S. Geological Survey (USGS) on salinity and selenium loads and trends in the lower Gunnison River Basin have focused primarily on concentrations at main-stem sites along the Gunnison River (Butler and Leib, 2002; Thomas and others, 2008; Mayo and Leib, 2012; Schaffrath, 2012). The Smith Fork Creek region, in the North Fork of the Gunnison River Basin and part of the Lower Gunnison Basin Unit, is a significant tributary to the Gunnison River but has little to no historical salinity or selenium data (Bureau of Reclamation, 2009a).

The Bureau of Reclamation (Reclamation) and the Natural Resources Conservation Service (NRCS) are responsible for assessing and implementing measures to reduce salinity and selenium loading in the Colorado River Basin. As part of this process, cost-sharing programs are used to involve the agricultural community in salinity reduction efforts. These cost-sharing programs help farmers, ranchers, and canal companies improve the efficiency of water delivery systems and irrigation practices. The delivery systems (irrigation canals) have been identified as potential sources of seepage, which can contribute to salinity loading (Bureau of Reclamation, 1982). Reclamation wants to identify seepage from irrigation systems in order to maximize the effectiveness of various salinity-control methods, such as polyacrylamide lining and piping of irrigation canal programs. Certain salinity control units (the Grand Valley and the Uncompahgre Project region of the lower Gunnison River Basin) have been extensively studied by Reclamation and NRCS, and Reclamation completed an intensive study of the lower Gunnison River Basin in the late 1970s. The resulting document (“Lower Gunnison Basin Unit—Feasibility Report” [Bureau of Reclamation, 1982]) summarizes the condition of the Lower Gunnison Basin Unit and is a benchmark study for salinity loading in the unit. However, some areas of the Lower Gunnison Basin Unit have limited data available for prioritizing salinity-control efforts. Additional data are required in these data-poor regions to make reasonable estimates of salinity loads and salinity-control efforts.

The Colorado State water-quality standard for dissolved selenium is 4.6 micrograms per liter ($\mu\text{g/L}$) (Colorado Department of Public Health and Environment, 1983). Elevated selenium concentrations in many western Colorado streams and tributaries have resulted in the placement of many streams and tributaries on the U.S. Environmental Protection Agency’s 303(d) list of impaired waters. Identifying the potential source areas of dissolved selenium loading can provide valuable information on where improvements can be made to reduce the levels of dissolved selenium.

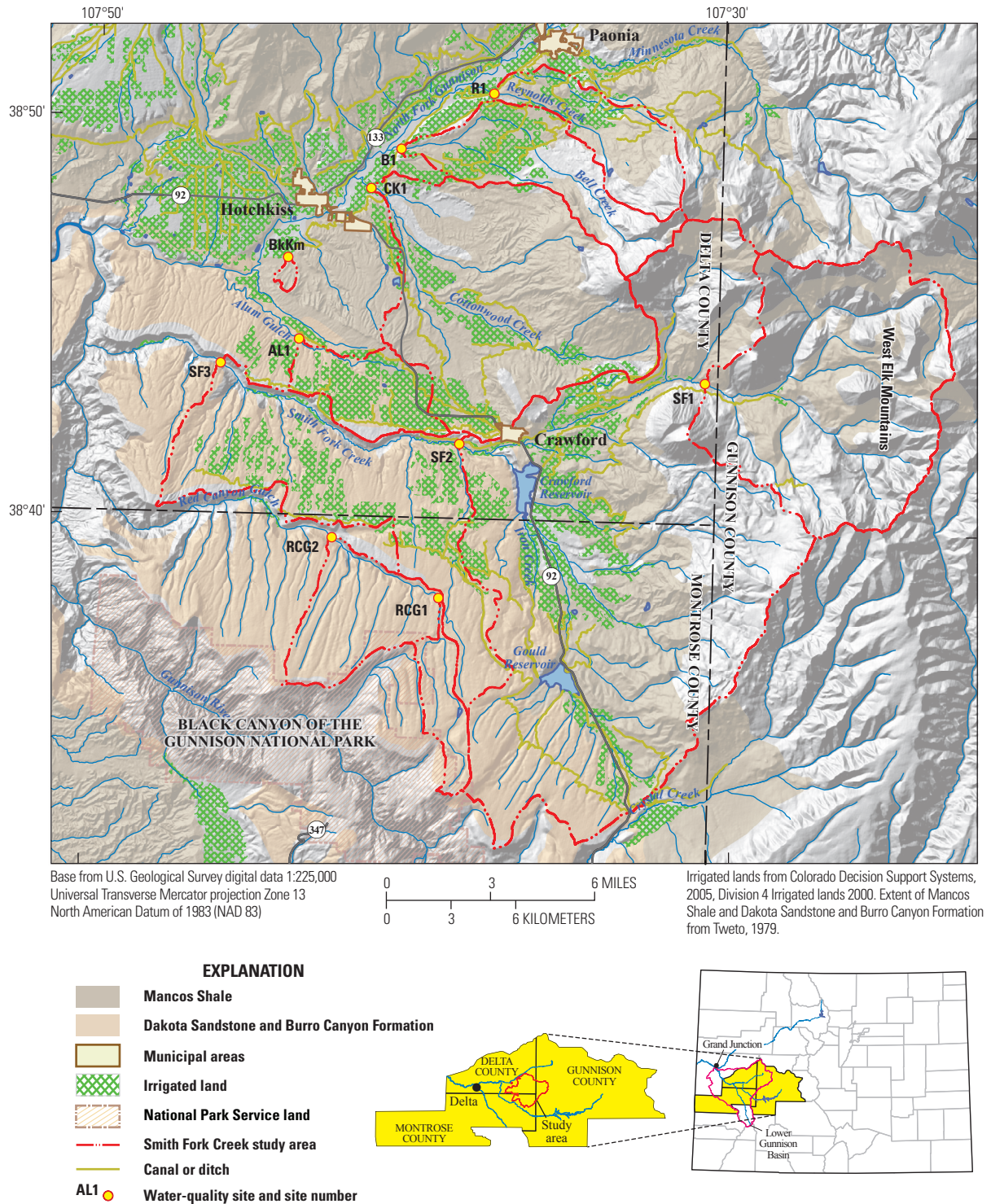
The Smith Fork Creek region is one of the most data-poor regions in the Lower Gunnison salinity control unit. The Smith Fork Creek region, herein referred to as the study area, comprises seven streams—Alum Gulch, Bell Creek, Cottonwood Creek, Reynolds Creek, Red Canyon Gulch, Smith Fork Creek, and one unnamed stream. Because little is known about the potential salinity and selenium loading associated with the Smith Fork Creek region, the USGS, in cooperation with Reclamation, developed a study to characterize the salinity and selenium loading there. This study will help identify where control efforts can be maximized to reduce salinity and selenium loading.

Purpose and Scope

The study area consists of 10 subbasins—Alum Gulch, Bell Creek, Cottonwood Creek, Reynolds Creek, Red Canyon Gulch 1, Red Canyon Gulch 2, Smith Fork Creek 1, Smith Fork Creek 2, Smith Fork Creek 3, and an unnamed stream. The purpose of this report is to (1) characterize the total annual salinity loads for each subbasin, (2) characterize the groundwater component of each subbasin, (3) characterize the natural salinity load for each subbasin, (4) characterize the on-farm and off-farm salinity loads for each subbasin, (5) calculate a selenium/salinity load ratio for each subbasin, and (6) estimate and report the total annual salinity and selenium loads for the study area. Subbasins were selected based on their location to Smith Fork Creek, canal network, type of land use, and potential for salinity and selenium loading to the lower Gunnison River Basin. Streamflow and water-quality data were collected during the period April 2008–March 2009 to characterize salinity and selenium loading in each subbasin. Streamflow was measured using standard current-meter methods. Canal specific conductance was measured using a specific conductance meter on five occasions from March 2008 to December 2008. Well data near specified canals were collected to help distinguish the off-farm salinity load. The sample data were analyzed, and salinity and selenium load are discussed within this report.

Description of Study Area

The Smith Fork Creek region of the lower Gunnison River Basin is in Delta, Gunnison, and Montrose Counties (fig. 1). The study area is south of the North Fork of the Gunnison River and south to southeast of the municipalities of Hotchkiss and Paonia. The municipality of Crawford is within the study area (fig. 1). The 2008 census identifies the populations of Hotchkiss, Paonia, and Crawford as 1,084, 1,633, and 392, respectively (U.S. Census Bureau, 2009). The southwest border of the study area is adjacent to the Black Canyon of the Gunnison National Park, and the eastern edge of the study area lies within the West Elk Mountains, which serve as the headwaters to the study area (fig. 1). The study area comprises a wide range of elevations, from approximately 12,000 feet (ft) in the headwaters to approximately 5,000 ft



at the confluences with the North Fork of the Gunnison River (ESRI, 2010). Irrigated land was calculated using the spatial analyst tool in ARCGIS from the Colorado's Decision Support System (2005), Division 4 Irrigated Lands 2000 base layer and comprises approximately 26,500 acres of the 327,000-acre study area (ESRI, 2010). An extensive irrigation system of canals and ditches has been developed to deliver water to the study area from Smith Fork Creek, the North Fork of the Gunnison River, and Crystal Creek (fig. 1, shown in yellow). Most of the fields are irrigated with either gated-pipe or flood irrigation; there are few sprinkler systems in the area. Inefficient irrigation methods can potentially cause an increase in salinity loads attributed to excessive deep percolation.

Climate and Hydrology

The climate of the study area is semiarid to temperate (Western Regional Climate Center, 2014). The range of precipitation (estimated with the Parameter-elevation Regressions on Independent Slope Models [PRISM] system; Daly and others, 1994) within the study area reflects the variability of the climate. The high-elevation headwaters received an estimated 22.5 inches (in.) of precipitation for the study period, whereas lower-elevation areas of the study area received an estimated 10 in. of precipitation for the study period (Daly and others, 1994). Long-term record at USGS streamflow-gaging station 09152500 Gunnison River near Grand Junction, CO, indicates wetter than normal conditions by approximately 19.4 percent during water year 2008–water year 2009 (U.S. Geological Survey, 2010). The 19.4 percent wetter than normal condition was determined to be representative of the average condition in the lower Gunnison River Basin during the study period; however, individual basins within the lower Gunnison River Basin could have been wetter or dryer than what was seen at gaging station 09152500. For the purposes of this report, the 19.4 percent wetter than normal condition was used for adjustments to average conditions.

Annual snowmelt is the main source of streamflow throughout the year. Winter precipitation stored in the high-elevation regions as snowpack begins to melt in the late spring and early summer, causing streamflows to peak in May or June. Higher flows from melting snowpack are captured by two reservoirs in the study area: Crawford Reservoir, live capacity (reservoir capacity that can be withdrawn by gravity) of 14,120 acre-feet (acre-ft) (Bureau of Reclamation, 2009b), and Gould Reservoir (also known as Fruitland Mesa Reservoir), live capacity of 8,100 acre-ft. The reservoirs supply irrigation water throughout the year as snowmelt and precipitation become limited. Higher flows in streams begin to recede by early summer and then remain stable as irrigation water returns to the stream systems. At the end of October, irrigation is turned off for the season and streamflow declines until a base-flow condition is reached. Base-flow conditions remain until snowmelt returns. The previously discussed streamflow pattern is typical of most of the streams in the study area, with some exceptions; streams that do not receive

additional water throughout the season from irrigation systems tend to be ephemeral and only have streamflow during periods of snowmelt or rainfall (Butler and Leib, 2002).

Groundwater in the study area is associated with an alluvial aquifer and has varying water quality. The West Elk Mountains to the east are part of an extensive Tertiary igneous aquifer and help supplement base flow in the headwaters of the study area (Topper and others, 2003). There are numerous domestic and livestock wells in the region (typically along the North Fork of the Gunnison River) and numerous springs that drain into the surface-water system. Depending on the quality of discharging groundwater, surface-water quality can be affected.

Geology

The geology of the study area changes considerably from east to west. The West Elk Mountains to the east are igneous intrusive and extrusive rocks of Tertiary age and are associated with widespread volcanic activity that began around 36 million years ago. Many of the rocks in the West Elk Range are made of breccias and welded tuff (Hansen, 1987). The primary underlying geologic formations in the study area are the Cretaceous age Mancos Shale in the east and the Dakota Sandstone and Burro Canyon Formation in the west.

The Mancos Shale is a significant contributor of salinity to water systems where it is present. Deposition in a marine setting increases the abundance of Cl^- , Na^+ , Mg^{2+} , SO_4^{2-} , Ca^{2+} , K^+ , HCO_3^- , and CO_3^{2-} (Garrels and Thompson, 1962). Shale deposits tend to contribute more soluble ions than associated sandstone marine deposits and present a higher salinity source. Conversely, alluvium that has been transported and deposited in a fluvial system has had most of its soluble ions removed and does not contribute as much salinity as bedrock shale deposits (Laronne, 1977). The Mancos Shale also contains appreciable amounts of gypsum, which is the dominating soluble mineral in the shale, but high amounts of sodium and magnesium hydrate sulfates also are present. Salt crusts (also known as effervescent salts and evaporative facies) are significant contributors of salts during precipitation runoff events. The salt crusts are formed from the evapoconcentration of dissolved solids after transport to the soil surface. Shale bedrock has low permeability and overland flow does not readily percolate into the soil, which allows for evaporation of water and precipitation of dissolved solids and the development of salt crusts (Laronne, 1977).

Data Collection and Analysis

Streamflow and water-quality data were collected by the USGS at 10 sites in the study area during the period April 2008–March 2009. The data collection stations were established at 10 sites on Alum Gulch, Bell Creek, Cottonwood Creek, Red Canyon Gulch (2 sites), Reynolds Creek, Smith Fork Creek (3 sites), and one unnamed stream.

Water temperature, gage height, and specific conductance were recorded at 15-minute intervals at each of the sites using a YSI 600LS water-quality sonde using standard techniques described in Wagner and others (2006). Streamflow was measured using a YSI FlowTracker Acoustic Doppler Velocimeter (ADV) and standard techniques described within Turnipseed and Sauer (2010). Six water-quality samples also were collected at each site during the study. The samples were analyzed for major ions and selenium concentration. Specific conductance was also measured at 12 irrigation canal sites using a YSI 30 handheld conductivity and temperature meter (2 to 6 times) during the study period. Two sites were selected on Red Canyon Gulch, dividing the subbasin into an upper subbasin, Red Canyon Gulch 1 (RCG1), and a lower subbasin, Red Canyon Gulch 2 (RCG2) (fig. 1). Subbasins RCG1 and RCG2 are considered natural sandstone sites for this study.

Smith Fork Creek was divided into three subbasins. The upstream site, Smith Fork Creek 1 (SF1), is upstream of irrigation activity and is one of four natural sites used in the study. Smith Fork Creek 2 (SF2) is approximately 1 mile (mi) to the west of Crawford and includes all streams that drain into Smith Fork Creek to the south of Crawford, including Iron Creek and its tributaries. Smith Fork Creek 3 (SF3) is approximately 2 mi upstream of the confluence with the Gunnison River and includes the remaining portion of the Smith Fork Creek drainage (fig. 1, table 1).

The sites on Alum Gulch (AL1), Bell Creek (B1), Cottonwood Creek (CK1), and Reynolds Creek (R1) were located as close to the mouth of the respective stream as possible to maximize the monitored drainage area. The unnamed stream (BkKm) is ephemeral and typically flows during snowmelt and convective rain storms. It was selected for its representative size, land use, and geology type: subbasin BkKm is small, has no irrigation, and is completely within Mancos Shale geology (fig. 1).

Sampling and Data Analysis

Water-quality samples were collected every 8 weeks during the period April 2008–March 2009, resulting in a total of six samples per site for the study period. Sample collection protocols and procedures followed USGS protocols found in the “National Field Manual for the Collection

of Water-Quality Data” (U.S. Geological Survey, variously dated). Most stream samples were collected as a grab sample because streams were quantified as being well-mixed. Water-quality samples were collected at approximately the same time that streamflow was measured.

Water-quality samples were collected in 3-liter (L) polyethylene bottles and filtered with a 0.45-micrometer (μm) capsule filter into 250-milliliter (mL) polyethylene bottles for laboratory analysis. Nitric acid was used to preserve water-quality samples for cation and trace metal analysis. All samples were collected and processed while wearing powderless surgical gloves to prevent contamination during handling. Laboratory analysis was conducted at the USGS National Water Quality Lab (NWQL) in Lakewood, Colo., following methods described by Fishman and Friedman (1989). Quality assurance and quality control (QA/QC) was conducted by collecting quality-control samples throughout the study period. Five QA/QC samples were collected consisting of three replicate samples and two blank samples. The QA/QC samples were sent to the NWQL and analyzed by methods described in the NWQL QA/QC manual (Pritt and Raese, 1992). Approximately 10 percent of the samples collected during the study period were QA/QC samples. Data from QA/QC samples were used in analysis of errors in load estimations.

Water Budget

A water budget for the study period April 2008–March 2009 was calculated for each subbasin using precipitation estimates, gaged surface-water flows (streamflow), evapotranspiration estimates, and estimated groundwater volumes. The PRISM system (Daly and others, 1994) was used to estimate precipitation inputs to each subbasin for each month of the study period (from a 4-kilometer grid resolution). Gaged streamflow at each site was quantified using a rating curve developed for each water-quality site based on the six streamflow measurements and the correlated stream-water level (Rantz and others, 1982). It was assumed the gaged streamflow originated from both groundwater inflow and surface-water runoff. Both streamflow components were considered in the estimation of the water and salinity budgets. Daily mean streamflows were estimated for each day in the study period from the 15-minute data and then summed to

Table 1. U.S. Geological Survey (USGS) water-quality data collection sites in the study area, April 2008–March 2009.

USGS site identification	Site name	Site number (figure 1)	Latitude	Longitude
384434107432701	Alum Gulch near Hotchkiss, Colorado.	AL1	38°44'34"	107°43'27"
384922107402001	Bell Creek at county road and railroad tracks, near mouth	B1	38°49'22"	107°40'20"
384633107435301	North Fork Gunnison River tributary near Hotchkiss, Colorado.	BkKm	38°46'33"	107°43'53"
384822107411201	Cottonwood Creek at County Road J75, near mouth	CK1	38°48'22"	107°41'12"
385049107372402	Reynolds Creek near Paonia, Colorado	R1	38°50'49"	107°37'24"
383809107384501	Red Canyon Gulch at Poison Spring Gulch near Crawford, Colorado	RCG1	38°38'09"	107°38'45"
383934107421501	Red Canyon Gulch near Trail Gulch near Crawford, Colorado	RCG2	38°39'34"	107°42'15"
09128500	Smith Fork Creek near Crawford, Colorado	SF1	38°43'40"	107°30'22"
384200107381401	Smith Fork Creek at 38.5 Road bridge near Hotchkiss, Colorado	SF2	38°42'00"	107°38'14"
384345107453801	Smith Fork Creek above mouth near Black Canyon	SF3	38°43'45"	107°45'38"

estimate a total streamflow for the study period. Surface-water volume estimates entering and exiting each subbasin by canal were determined from field-level reconnaissance conducted by the Irrigation Water Management Specialist of the Delta Conservation District (Delta Conservation District, written commun., 2010).

Consumptive use rates for native vegetation and irrigated crops were estimated for each subbasin. Vegetation reference evapotranspiration (ET) was estimated by the Colorado Agricultural Meteorological network (CoAgMet) weather station, which reports a daily reference ET rate in inches per day. Data from CoAgMet weather station hot01 (CSU Rogers Mesa Expt Sta, located just to the northwest of the study area near Hotchkiss) were summed to estimate a monthly reference ET during the period April 2008–March 2009 (Colorado State University, 2009). Native vegetation consumptive use was estimated using the Penman-Montieth method (Allen and others, 1998). Crop coefficients for native vegetation in the arid western United States were obtained through the New Mexico Climate Center (2009). The crop coefficients were then multiplied by the reference ET and number of vegetated acres to achieve acre-feet per month.

Evapotranspiration rates for irrigated lands were estimated using the relation of potential ET to amount of water applied. Crops generally transpire at a maximum rate when soil remains at field capacity, and significant decreases are not typically seen until soil moisture falls below 50 percent of field capacity (Broner and Schneekloth, 2003). Hence, if the required amount of water for optimal growth is applied, the crop will evapotranspire (consumptive use) at its maximum potential rate; if less water is applied to prevent optimal growth, the consumptive use rate is reduced to maintain the relation. Broner and Schneekloth (2003) report consumptive use for various crops across western Colorado. An average consumptive use of crops near Gunnison, Colo., and Fruita, Colo., was used as an estimated consumptive use for the Smith Fork Creek region. The resulting consumptive use values were reported in acre-feet based on the number of acres of irrigated land in each subbasin.

In order to estimate the ungaged groundwater discharge from each subbasin, a water budget equation was developed using the following inputs and outputs:

$$Q_{GW} = (Q_{CI} + Q_P + Q_{GI}) - (Q_{CO} + Q_{CCU} + Q_{OCU} + Q_{SW}) \quad (1)$$

where

- Q_{GW} is the estimated rate of ungaged groundwater discharge for each subbasin, in acre-feet per year;
- Q_{CI} is the rate of canal water diverted into the subbasin, in acre-feet per year;
- Q_P is the estimated precipitation, in acre-feet per year;
- Q_{GI} is the rate of gaged streamflow that enters the subbasin, in acre-feet per year;
- Q_{CO} is the rate of canal water diverted out of the subbasin, in acre-feet per year;

Q_{CCU} is the estimated rate of crop consumptive use, in acre-feet per year;

Q_{OCU} is the estimated rate of other consumptive use (natural consumptive use, phreatophyte consumptive use, municipal consumptive use, and open water consumptive use), in acre-feet per year; and

Q_{SW} is the rate of gaged streamflow minus base flow, in acre-feet per year.

The rate of gaged streamflow minus base flow (Q_{SW}) is determined by

$$Q_{SW} = Q_g - Q_B \quad (2)$$

where

Q_g is the rate of gaged streamflow at the surface-water gage, in acre-feet per year; and

Q_B is the annual volume of base flow at the surface-water gage, in acre-feet per year.

The annual volume of base flow (Q_B) is in turn determined by

$$Q_B = \frac{L_G - C_{SW}Q_gK}{(C_B - C_{SW})K} \quad (3)$$

where

L_G is the annual salinity load at the surface-water gage, in tons per year;

C_B is the base-flow salinity concentration (November 1–March 31) at the surface-water gage, in milligrams per liter;

C_{SW} is the annual streamflow concentration, in milligrams per liter; and

K is the unit conversion factor to obtain tons per year from milligrams per liter and acre-feet per year.

For this analysis, because there was no groundwater monitoring network in place to verify any changes occurring in the groundwater system, it was assumed that there was no change in storage for each subbasin during the study period. Assuming no change in groundwater storage, equation 1 could be solved for the rate of ungaged groundwater. Therefore, the groundwater volume for each subbasin was estimated to be the remaining volume after the outputs, ($Q_{CO} + Q_{CCU} + Q_{OCU} + Q_{SW}$), were subtracted from the inputs, ($Q_{CI} + Q_P + Q_{GI}$). The estimated surface-water and groundwater volumes could then be used to estimate surface-water and groundwater salinity loads. Note that estimated groundwater volumes are specific to the period of study and likely some storage occurred but could not be measured without a groundwater monitoring network in place specific to each subbasin. As a result, the assumption of zero change in storage implies all groundwater from this method had the potential to load salinity and selenium to streams in the study area. In reality, some of the groundwater was likely retained as storage, thus the loads in certain subbasins for the study period may have been over estimated.

Salinity Budget

A salinity budget was developed for each subbasin to quantify the sources of salinity. A simplified form of a salinity budget is the total salinity load equal to the surface-water salinity load plus the groundwater salinity load. This simplified equation is effective at quantifying the total salinity load, but it does not differentiate the salinity loading sources. To estimate the different sources of the total salinity load, the following modified equation was used:

$$T = F_{on} + F_{off} + N + M \quad (4)$$

where

- T is the total salinity load for each subbasin, in tons per year;
- F_{on} is the estimated on-farm (deep percolation plus tail water) salinity load for each subbasin, in tons per year;
- F_{off} is the estimated off-farm (canal seepage) salinity load for each subbasin, in tons per year;
- N is the estimated natural salinity load for each subbasin, in tons per year; and
- M is the estimated municipal salinity load for each subbasin, in tons per year.

Surface-water salinity loads for each subbasin were estimated based on data collected at each water-quality monitoring site. Specific conductance normalized to 25 °C and water-level measurements were collected every 15 minutes. The gage-height measurements were used to estimate

streamflow based on a rating for each site (table 2). Continuously measured values of specific conductance (every 15 minutes) were converted to salinity concentrations (total dissolved solids [TDS]; Hem, 1989) based on the linear relation between the calculated total dissolved solids concentrations in water-quality samples and the corresponding observed specific conductance values from the continuous monitors (table 3) (Hem, 1989). Salinity loads for each 15-minute interval were estimated using the following equation:

$$L = Q_{cfs} \times TDS \times 0.000028 \quad (5)$$

where

- L is the salinity load, in tons per 15 minutes;
- Q_{cfs} is the streamflow, in cubic feet per second;
- TDS is the total dissolved solids concentration, in milligrams per liter; and
- 0.000028 is the conversion factor to convert to tons per 15 minutes.

The 15-minute load estimations were aggregated to daily loads and monthly loads. The monthly loads were summed to estimate a gaged surface-water load for the study period April 2008–March 2009.

Groundwater salinity loads were calculated for each subbasin based on equation 1. If a negative groundwater discharge was calculated, then it was assumed that an unmeasured inflow source of water was present, thereby giving the impression of a net loss in the groundwater system. This phenomenon only occurs at two subbasins in the study area, SF1 and BkKm. Subbasin SF1 is situated in a Tertiary volcanic aquifer system. This system is highly fractured and may serve as a conduit

Table 2. Summary of gage height to streamflow ratings at selected sites in the study area, April 2008–March 2009.

[AL1, Alum Gulch; B1, Bell Creek; BkKm, North Fork Gunnison River tributary (background Mancos Shale site); CK1, Cottonwood Creek; R1, Reynolds Creek; SF1, Smith Fork Creek near Crawford, CO; SF2, Smith Fork Creek at 38.5 Road bridge near Hotchkiss, CO; SF3, Smith Fork Creek above mouth near Black Canyon; RCG1, Red Canyon at Poison Springs Gulch; RCG2, Red Canyon near Trail Gulch; lnQ, natural logarithm of streamflow; lnD, natural logarithm of gage height; R², coefficient of determination; RSE, residual standard error¹; --, no data]

Site number	Equation	Coefficient	Y-intercept	R ²	RSE
AL1	$\ln Q = 0.9319(\ln D) + 2.8825$	0.9319	2.8825	0.90	0.2884
B1	$\ln Q = 6.7248(\ln D) - 8.6407$	6.7248	-8.6407	0.84	0.2933
BkKm	--	--	--	--	--
CK1	$\ln Q = 0.7983(\ln D) + 2.4044$	0.7983	2.4044	0.93	0.1719
R1	$\ln Q = 1.3328(\ln D) + 0.6138$	1.3328	0.6138	0.67	0.2960
RCG1	$\ln Q = 2.7059(\ln D) + 0.1894$	2.7059	0.1894	1	0
RCG2	$\ln Q = 0.36(\ln D) - 4.932$	0.36	-4.932	1	0
SF1	$\ln Q = 11(\ln D) - 12.247$	11	-12.2470	0.96	0.3900
SF2	$\ln Q = 2.2774(\ln D) + 3.3805$	2.2774	3.3805	0.95	0.6034
SF3	$\ln Q = 12.8264(\ln D) - 20.8348$	12.8264	20.8348	0.94	0.5039

¹Helsel and Hirsch (2002).

Table 3. Summary of equations for estimating total dissolved solids for specific conductance in agricultural and natural subbasin types.

[TDS, total dissolved solids; SC, specific conductance; R², coefficient of determination]

Subbasin type	Equation	Coefficient	Y-intercept	R ²
Agricultural	$TDS = 0.8499(SC) - 101.27$	0.8499	-101.27	0.99
Natural	$TDS = 0.5228(SC) + 9.384$	0.5228	9.384	0.96

for groundwater inflow from adjacent subbasins, which might explain why the subbasin SF1 “outputs” exceed the “inputs.” Streamflow in subbasin BkKm also did not appear to have a groundwater component according to water balance estimates. The subbasin is small and located in lower elevations of the study area where precipitation is low. Additionally, only one streamflow event from a rain storm was recorded during the study period, limiting a robust evaluation of subbasin BkKm.

To estimate the salinity load associated with the groundwater discharge, it was necessary to estimate the salinity concentration of the groundwater. Salinity concentrations were estimated using the average salinity (TDS) concentration for the base flow during the months November through March (nonirrigation season). To estimate the groundwater concentration at sites that had no base flow, historic samples from groundwater wells located in or near the desired subbasin were used. Subbasins RCG1 and RCG2 were the only sites that had a groundwater component but no measured base flow. Analysis of a sample collected from a USGS well (station number 384005107401001; station name NB05100720DBD1) was used to estimate the groundwater TDS concentration in the Dakota Sandstone (U.S. Geological Survey, 2013). Average base-flow TDS concentrations for each subbasin can be found in table 4.

Groundwater salinity loads were calculated using the following equation:

$$L_{GW} = Q_{Acre-ft} \times C_{lf} \times 0.00136 \quad (6)$$

where

L_{GW} is the salinity load of the groundwater, in tons per year;

$Q_{Acre-ft}$ is the estimated groundwater discharge, in acre-feet per year;

C_{lf} is the groundwater salinity concentration, in milligrams per liter; and

0.00136 is the conversion factor to convert to tons per year.

To adjust for salinity load associated with canals moving water across subbasin boundaries, salinity loads were subtracted from the subbasins receiving the canal water and added back to the subbasins where the source waters originated. This adjustment ensured that subbasins providing irrigation water were responsible for canal salinity load and that the salinity load for subbasins receiving canal water from outside sources did not inaccurately include salinity loads originating in other subbasins.

Off-Farm Salinity Load Estimation

Heat-tracer investigations were completed at two sites to determine if these methods could provide quantitative salinity load estimates associated with canal seepage. The two site locations were not located in the Smith Fork Creek region because of restrictions to canal access and canal conditions at the time of the survey in late March 2010. The sites were located approximately 30 kilometers (km) to the west of the study area near Delta, Colo., and were considered representative of the study area based on the similar lithology and size of the canals. The first site, Kdb, is approximately 11 km southwest of Delta, Colo., and is in the Dakota Sandstone. The second site, Km, is about 10 km southeast of Delta, Colo., and is in the Mancos Shale (fig. 2). The two sites were chosen based on lithology, accessibility, and accommodating canal conditions (specifically, dry canal bed).

VS2DH Model Framework, Data Collection, and Calibration

The effectiveness of using heat as a tracer in groundwater and surface-water interaction studies has been well established. Heat tracer techniques have been applied successfully to determine streambed hydraulic conductivity (Essaid and others, 2007; Zamora, 2008; Eddy-Miller and others, 2009), assess diurnal and annual variability in groundwater/surface-water exchanges (Ronan and others, 1998; Cox and others, 2007), and determine groundwater recharge from ephemeral streams (Constantz and others, 2002). The practicality of using heat as a tracer has improved substantially in recent years because of improvements in data collection equipment and computational capabilities (Stonestrom and Constantz, 2003). For more detail on the use of this technique in studies of groundwater and surface-water interaction and groundwater transport, refer to Constantz and others (2002), Stonestrom and Constantz (2003), Andersen (2006), Blasch and others (2007), and Constantz (2008).

Numerical modeling of continuous sediment-temperature data allowed canal leakage to be quantified. The groundwater flow and transport model VS2DH (Healy and Ronan, 1996) was used to simulate flow and estimate the hydraulic conductivity of the canal bed sediment at the temperature monitoring sites. The VS2DH transport model is a finite-difference model that uses a modified version of the advection-dispersion equation expressed in terms of water temperature (Healy and Ronan, 1996). Flow through the unsaturated zone is solved using a modified version

Table 4. Calculated average base-flow concentrations of total dissolved solids for selected sites in the study area, April 2008–March 2009.

[AL1, Alum Gulch; B1, Bell Creek; BkKm, BkKm, North Fork Gunnison River tributary (background Mancos Shale site); CK1, Cottonwood Creek; R1, Reynolds Creek; SF1, Smith Fork Creek near Crawford, CO; SF2, Smith Fork Creek at 38.5 Road bridge near Hotchkiss, CO; SF3, Smith Fork Creek above mouth near Black Canyon; RCG1, Red Canyon at Poison Springs Gulch; RCG2, Red Canyon near Trail Gulch; TDS, total dissolved solids; --, no data available]

	AL1	B1	BkKm	CK1	R1	RCG1	RCG2	SF1	SF2	SF3
Average base-flow TDS concentration, in milligrams per liter	1,628	1,874	--	2,310	1,709	941	941	97.9	1,444	2,267

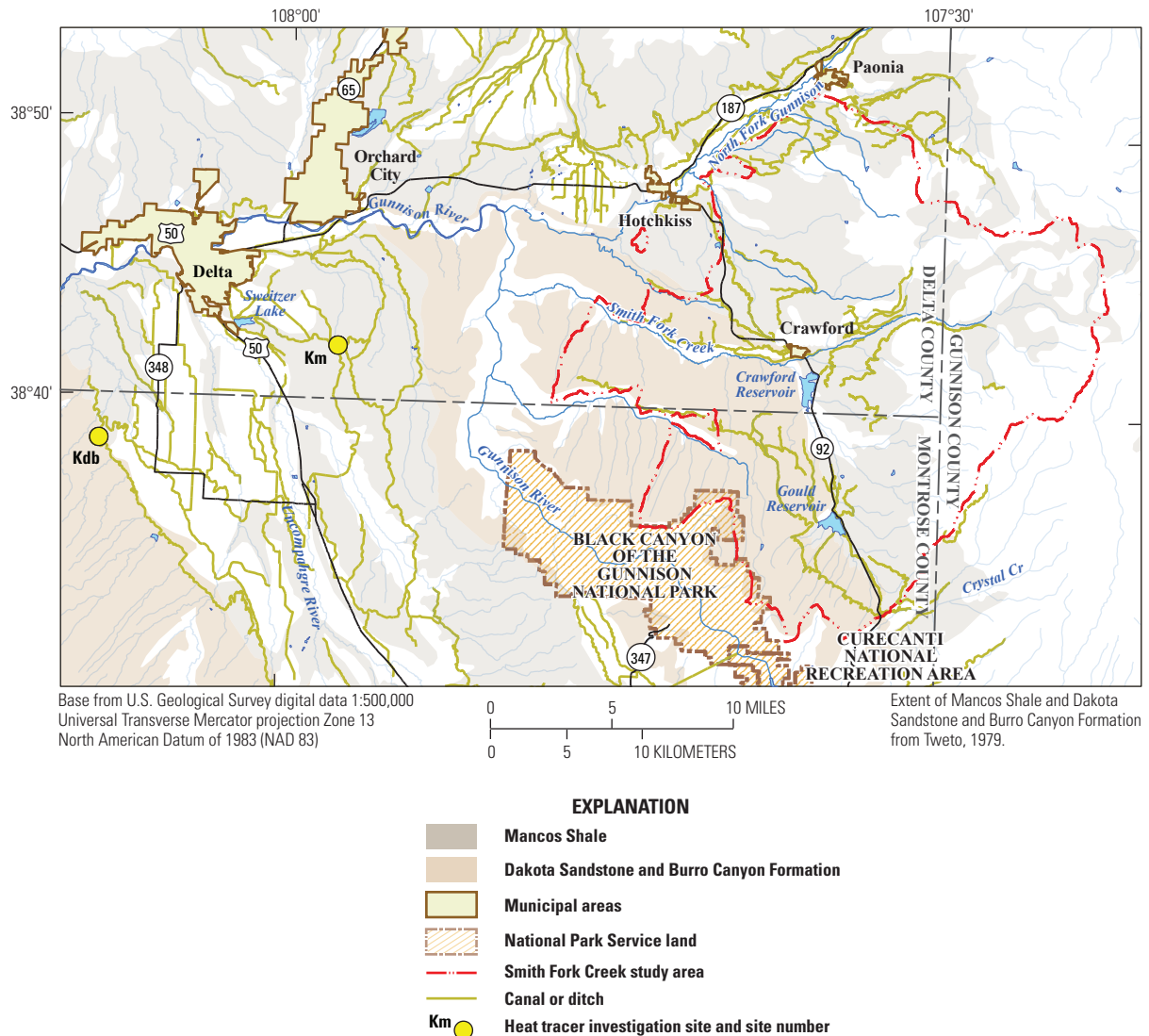


Figure 2. Location of heat-tracer investigations sites in relation to the study area.

of the Richards equation (Chow and others, 1988) that assumes hydraulic conductivity is a temperature-dependent variable because of viscosity effects. The VS2DH model required continuous records of the water temperature, canal stage, groundwater level, and sediment temperature at multiple depths beneath the canal bed (Stonestrom and Constantz, 2003).

Creating a VS2DH model involves specifying a model domain and boundary conditions that adequately represent the physical system at each temperature monitoring site. Model domains were created based on the physical characteristics unique to each site. Model domains for each VS2DH model were subdivided into a series of rows and columns, each assigned a sediment texture on the basis of the described lithology of continuous sediment cores collected at each temperature monitoring site. A sediment core was collected with each monitoring well that was installed; this typically consisted of a well in or as near as possible to the canal bottom and a second well located adjacent to the canal. Lithologic

descriptions of collected sediment cores are included in appendix 1 of this report. Estimates of thermal and hydraulic properties such as thermal conductivity of saturated sediment, porosity, and heat capacity of water were based on published values from Niswonger and Prudic (2003) and Healy and Ronan (1996).

The general model approach involved a period of investigation that was divided into 15-minute intervals called recharge periods, each having unique upper and lower boundary conditions based on measured water-level and water-temperature data. Model estimates of hydraulic conductivity of the canal bed sediment involved a trial-and-error approach to obtain the best fit between the simulated and measured sediment-temperature profiles. After each model simulation, the simulated temperatures from user-specified observation points were plotted and visually compared to the measured data from each corresponding depth. The hydraulic conductivity of the modeled sediment textures was adjusted

between simulations (trials) until the timing and amplitude of the diurnal temperature peaks agreed between the simulated and measured temperatures. Model parameters related to thermal properties were held constant for all the sediment textures used in each simulation and are summarized in table 5.

Data Collection—Mancos Shale Site Model

Water temperature, water-level, and specific conductance data were collected at site Km to enable the use of heat as a tracer to quantify the degree of groundwater and surface-water interaction. Canal bed sediment data were collected with a series of temperature loggers deployed inside of a stainless steel sand point. The HOBO temperature loggers were suspended at depths of 0.3 m, 0.46 m, and 0.61 m below the canal bed. Temperature loggers were deployed in March prior to the irrigation season and were retrieved and downloaded August 24, 2010. Canal-water temperature and stage were measured during the irrigation season with a YSI 600LS multiparameter sonde. The multiparameter sonde was deployed inside of a 4-in. polyvinyl chloride (PVC) stilling well with holes drilled to allow adequate exchange with the flowing water. Groundwater-level and temperature data were collected at two points beneath the canal with In-Situ Level TROLL® 700 data loggers with vented cable to the atmosphere. One Level TROLL 700 was deployed inside of a sand point driven 0.73 m into the canal bed (Km_well2). The screen interval was covered with pipe wrap except for the section from 0.40 m to 0.67 m below the canal bed, which was open to the surrounding sediments. A 2.0-m-long pipe was threaded to the top of the sand point above the water surface of the canal to allow proper venting for accurate pressure readings. Another Level TROLL 700 was placed at the bottom of a monitoring well (Km_well1) installed on a flat portion of the canal bank near the edge. The monitoring well was installed using a 2-in. geoprobe and cased with 1.25-in. PVC screened from 2.46 m to a maximum depth of 2.92 m. All continuous data collected at this site were recorded at 15-minute intervals throughout the duration of the study. A generalized diagram and map of the installation design for site Km is shown in figure 3.

Model Framework—Mancos Shale Site

A one-dimensional VS2DH model was constructed for the Km temperature monitoring site (fig. 2) based on the assumption of vertical flow below the canal. With this configuration, nonvertical (referred to hereafter as multidimensional) flow of water was ignored, and only the vertical hydraulic conductivity of the shallow bed sediment was estimated. The top boundary of the model was at the canal bed–water interface and was assigned specific-head and specific-temperature boundary conditions based on measured canal stages and canal water temperatures (see “Data Collection—Mancos Shale Site Model,” left). The bottom boundary was assigned specific-head and specific-temperature conditions on the basis of recorded groundwater levels and temperatures. The sides of the model domain were specified as no-flow boundaries. Model domains thus were to represent the subsurface from the canal-bed surface to the groundwater table before the irrigation season. The thickness of model domains were based on ground surface elevation data from surveyed topography collected at each site with a Sokkia SDL30 digital level with a vertical precision of 0.09 centimeters (cm). A generalized one-dimensional VS2DH model is shown in figure 4.

The VS2DH model domain extended from the elevation of the top of the canal bed to the water table elevation immediately before canal diversion. The entire model domain was uniformly subdivided into 100 rows and was assigned a 0.29-meter (m) unit of clay overlying 0.38 m of weathered Mancos shale based on data collected from well hole Km_well2 (fig. 3, appendix 1). The irrigation season was subdivided into 15-minute periods called recharge periods that had unique upper and lower boundary conditions. Canal-stage and water-temperature data were inputs for the upper boundary condition of each model simulation. The difference between the elevation of the canal bed and the elevation of the stage transducer in the stilling well (see “Data Collection—Mancos Shale Site Model,” left) were added to the stage record to determine the pressure head at the canal-bed surface.

Table 5. Calibrated VS2DH model parameters for simulation of hydraulic conductivity at heat-tracer test sites.

[Kzz/Khh, ratio of vertical (z) saturated hydraulic conductivity to horizontal (h) saturated hydraulic conductivity; Sat Khh, horizontal hydraulic conductivity; m/d, meters per day; cm³, cubic centimeters; RMC, residual moisture content; W/m °C, watts per meter degrees Celsius; J/m³ °C, Joules per cubic meter degrees Celsius; --, no data]

Model layer	Kzz/Khh	Sat Khh (m/d)	Porosity ¹ (cm ³ /cm ³)	RMC	alpha	beta	Thermal conductivity of saturated sediment ⁴ (W/m °C)	Heat capacity of water ⁵ at 20 °C (J/m ³ °C)
Km ¹ site								
Clay	--	6×10 ⁻⁶	0.38	0.38	--	--	2	4.2×10 ⁶
Weathered Mancos Shale	--	6×10 ⁻⁷	0.38	0.38	--	--	2	4.2×10 ⁶
Kdb ¹ site								
Silty clay	¹ 0.25	¹ 5×10 ⁻⁶	¹ 0.4	¹ 0.2	¹ 6	¹ 2	2	4.2×10 ⁶
Sandstone	² 0.67	² 1×10 ⁻⁸	² 0.25	² 0.2	³ 11	³ 2	2	4.2×10 ⁶

¹Meyer and others, 1997.

²Freeze and Cherry, 1979.

³V.M. Heilweil, U.S. Geological Survey, oral commun., November 12, 2010.

⁴Healy and Ronan, 1996.

⁵Niswonger and Prudic, 2003.

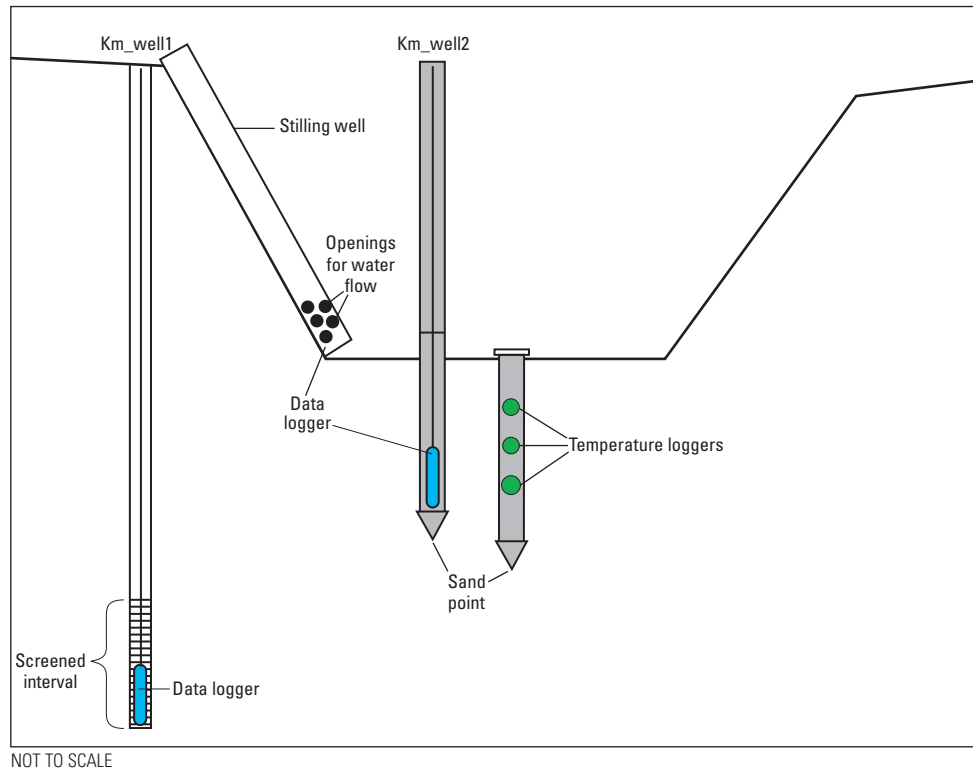


Figure 3. Generalized installation diagram for site Km.

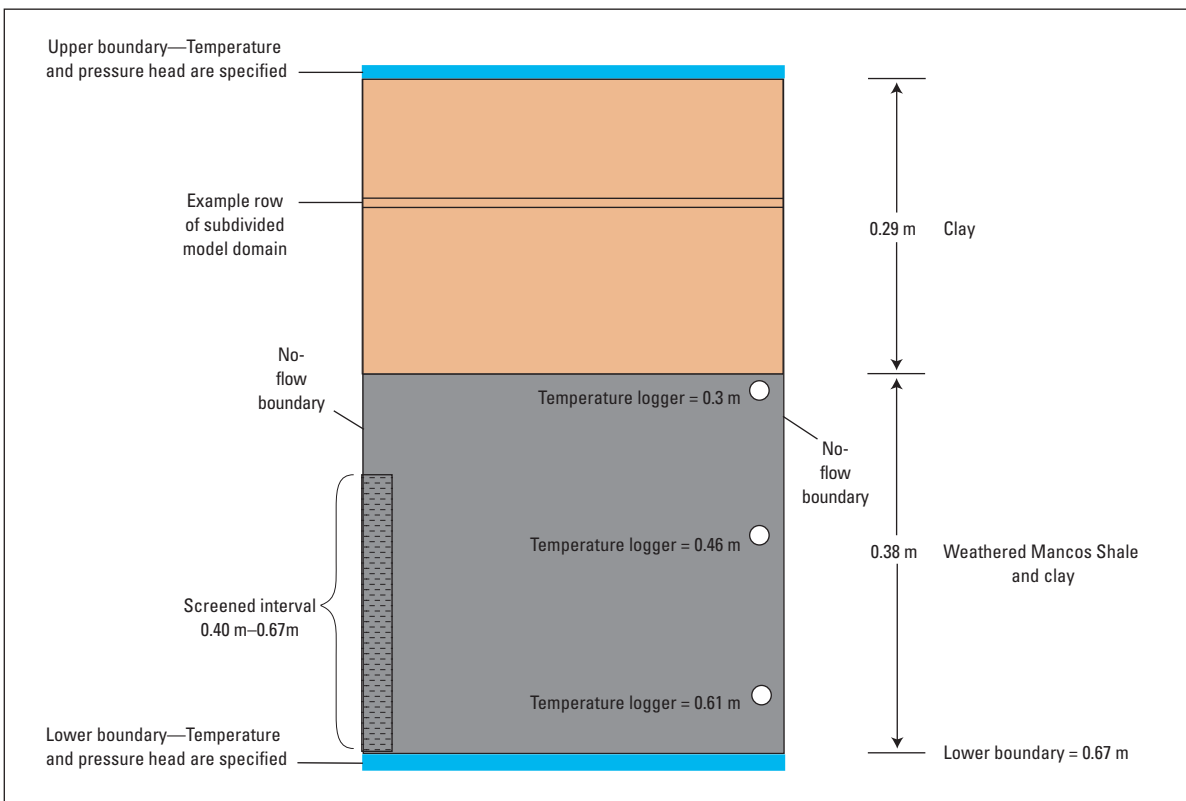


Figure 4. Generalized one-dimensional VS2DH model for site Km. (m, meter)

Continuous groundwater-level and groundwater-temperature data were inputs for the lower boundary condition of each model simulation. The water level was the pressure head exerted at the lower model boundary for each recharge period.

Model Calibration—Mancos Shale Site (Km)

Canal stage data indicate that diversion into the canal began on April 13; the Level TROLL 700 inside the sand point, however, did not begin recording data until May 7 because of a sensor malfunction. The water level recorded in the sand point displayed a high level of synchrony with the stage recorder, indicating a strong connection between the surface water and shallow groundwater (fig. 5*A, B*). The calculated vertical hydraulic gradient ranged from -1.06 meters per meter (m/m) to -0.64 m/m and was generally increasing towards the end of the period of record (fig. 5*C*). The recorded

water level in the deeper groundwater well increased gradually from the time of the installation and peaked on May 26, corresponding to the peak in canal stage. The slow response in water level measured in the well indicates a weak connection with the groundwater system.

Observed canal-water temperature ranged from 4.8 to 20.6 °C from the time of diversion to the end of the period of record. Diurnal canal-water temperature typically varied by 3 °C when flow was at or near maximum capacity (fig. 5*A*). Subsurface-temperature data generally reflected canal-water temperature data, but trends in temperature lagged and were dampened with depth. The magnitude of the diurnal variation in sediment temperature decreased with depth and was nonexistent below a depth of 0.46 m below the canal bed (fig. 6).

Hydraulic properties of site Km were estimated with a VS2DH model calibrated using field data. The vertical hydraulic conductivities of the sediment layers were estimated using

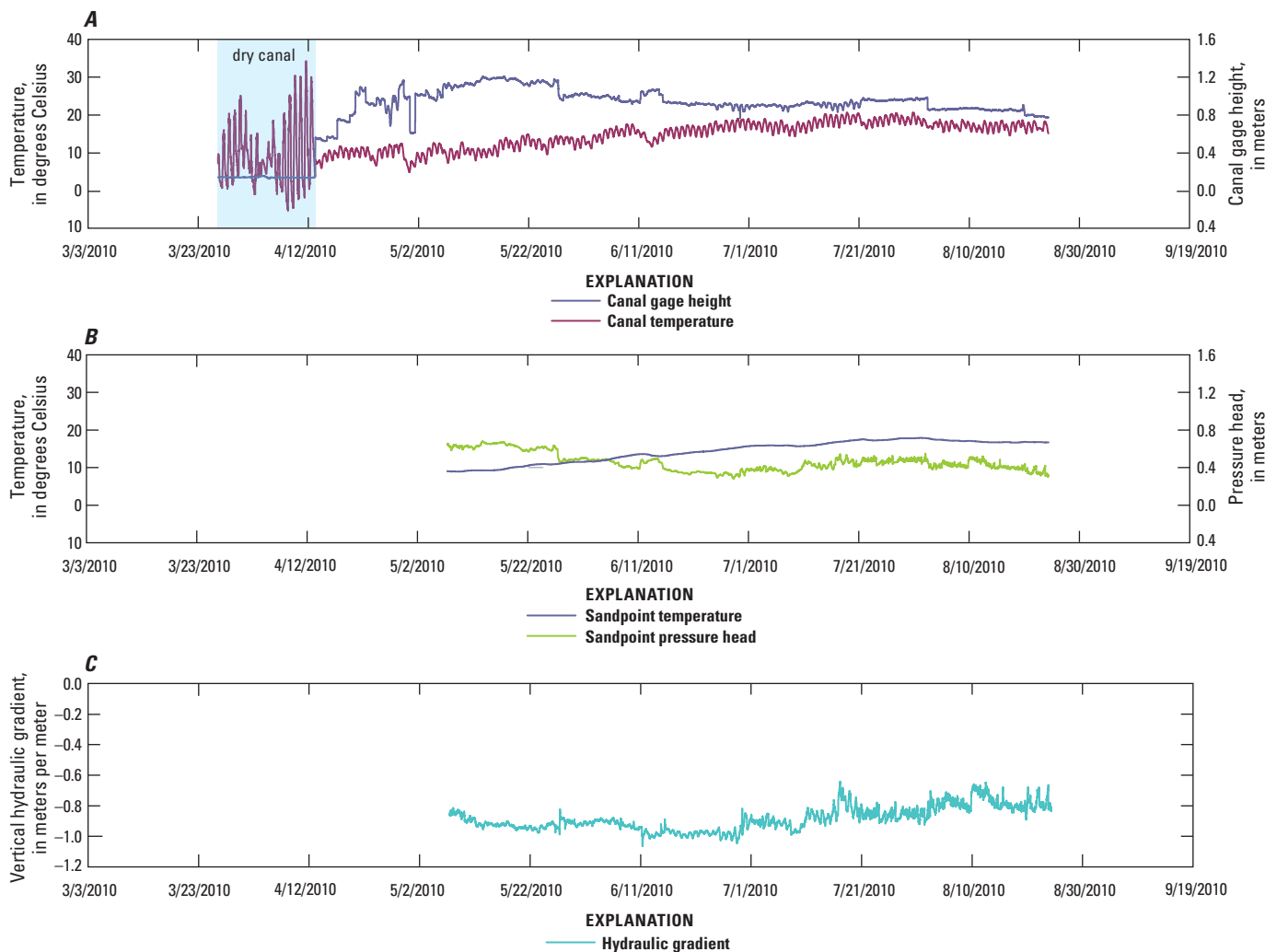


Figure 5. Observed temperature, gage height, pressure head, and hydraulic gradient at site Km. *A*, Canal gage height and temperature. *B*, Sandpoint temperature and pressure head. *C*, Vertical hydraulic gradient (negative values indicate downward flow from the canal into the canal bed).

a calibrated one-dimensional VS2DH model. Model simulations were begun only after the transducer in the sand point began recording data. After using a trial-and-error approach for calibration of pressure head and temperature, the average vertical hydraulic conductivities were estimated at 6×10^{-6} meters per second (m/s) for the clay unit and 6×10^{-7} m/s for the weathered Mancos shale unit. Measured and simulated subsurface temperatures are plotted in figure 6. Average vertical hydraulic conductivity of 1×10^{-6} m/s was computed from the harmonic mean of the modeled vertical hydraulic conductivities and sediment layer thicknesses (Healy and Ronan, 1996). This value is higher than what is published in Freeze and Cherry (1979) for shale, but extensive fracturing and weathering of the shale could allow for the higher hydraulic conductivities as modeled. Darcy's Law can be used to determine the daily canal seepage rate provided the average vertical hydraulic conductivity and hydraulic gradient are known.

Data Collection—Dakota Sandstone and Burro Canyon Formation Site Model

Water temperature, water-level, and specific conductance data were collected at site Kdb to enable the use of heat as a tracer to quantify the rates of leakage. The bed of the canal at site Kdb was made of competent, well-consolidated sandstone with evident fractures. The banks of the canal and overburden were composed of silty clay weathered from the underlying bedrock. The competent sandstone prevented coring beneath the canal bed and subsequent installation of instrumentation. To examine the potential lateral movement of water through the overburden, two sand points were driven into sediments at 3.8 and 8.2 m down-dip of the canal to the top of the well-consolidated sandstone. Each sand point was instrumented with an In-Situ Level TROLL 700 measuring subsurface temperature, water level, and specific conductance. Canal-water temperature and stage were measured during the

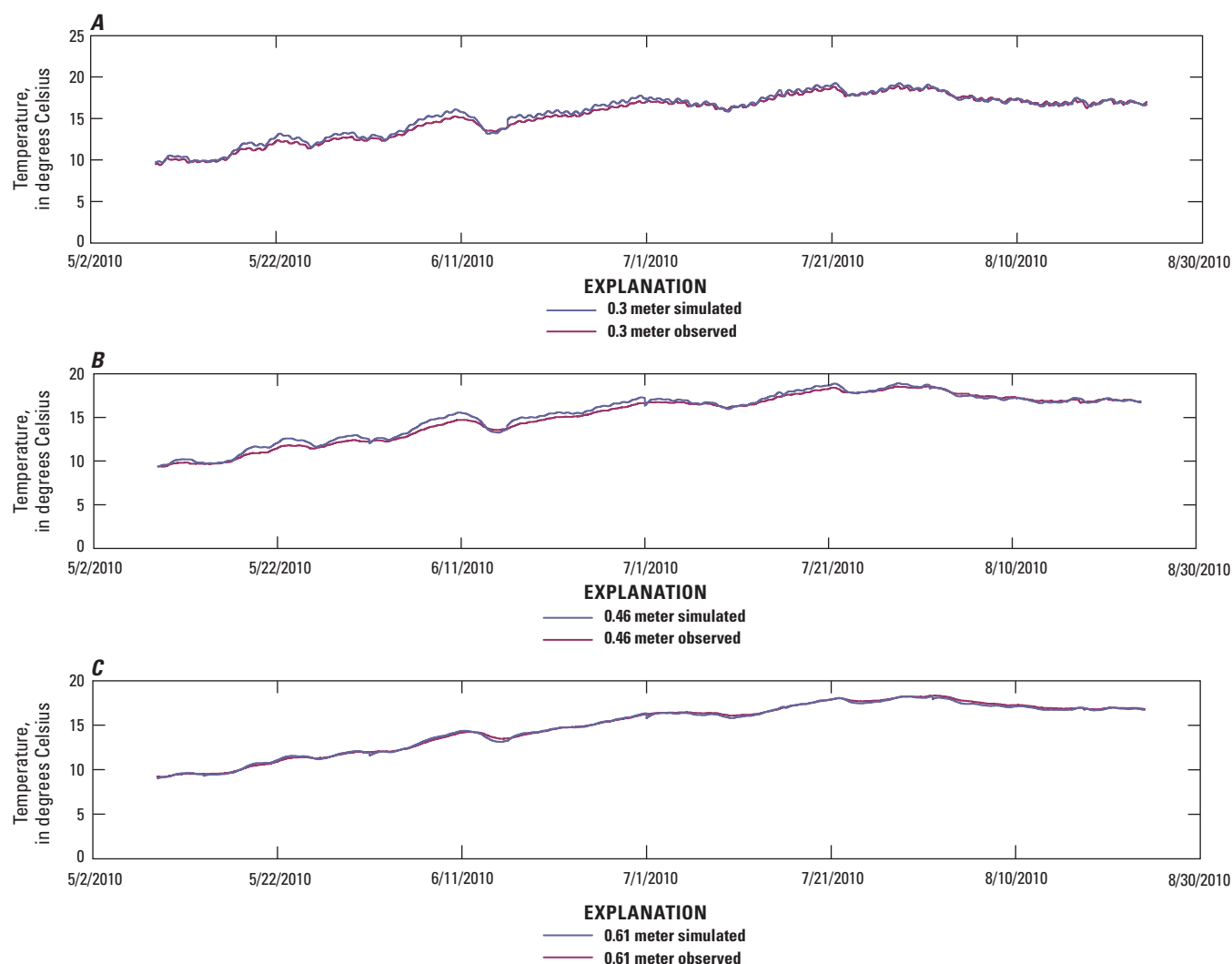


Figure 6. Observed and simulated subsurface temperature data at various depths below the canal bottom at site Km. A, 0.3 meters. B, 0.46 meters. C, 0.61 meters.

irrigation season with an YSI 600LS multiparameter sonde. The multiparameter sonde was deployed inside of a 4-in. PVC stilling well with holes drilled to allow adequate exchange with the flowing water. A generalized diagram of the installation design can be found in figure 7.

Model Framework—Dakota Sandstone and Burro Canyon Formation Site

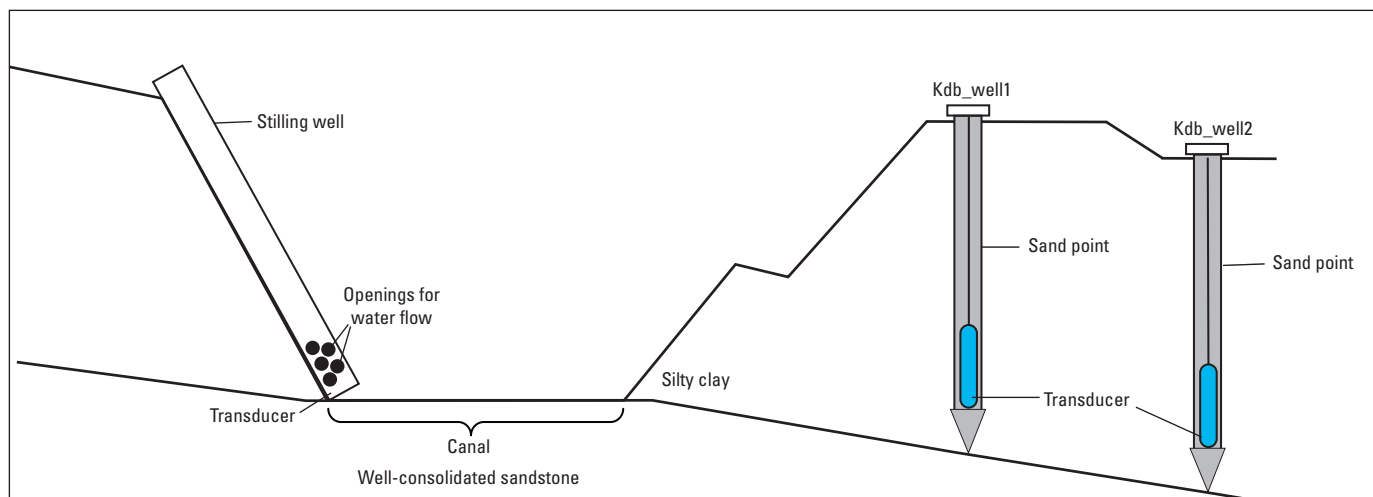
A two-dimensional VS2DH model was constructed for the Kdb temperature monitoring site based on the assumption that flow through canal bed sediment would be multi-dimensional and largely controlled by bedrock topography. Continuous sediment-core data indicate that approximately 1 m of silty clay overlies competent (bedrock) sandstone of the Burro Canyon Formation (appendix 1). The configuration of the model domains were based on ground surface elevation data from surveyed topography collected at each site with a Sokkia SDL30 digital level with a vertical precision of 0.09 cm. A generalized two-dimensional VS2DH model is shown in figure 8. The entire model domain was subdivided equally into 100 rows and 250 columns. The upper left part of the model domain was the right side of the canal bank and was subdivided into segments reflecting the surveyed topography. This part of the model domain was assigned boundary conditions based on the total head and daily temperature measured in the canal. The top boundary of the model was at the land surface and was given no-flow and specified temperature based on measured temperatures. The bottom boundary and the right side of the domain were assigned seepage faces. The lower left side of the model domain was specified as a no-flow boundary. The irrigation season was subdivided into 24-hour periods called recharge periods that had unique boundary conditions. Average daily canal-stage and water-temperature data were inputs for the upper boundary condition of each model simulation (see Data Collection—Dakota

Sandstone and Burro Canyon Formation Site Model section). Average daily air temperatures were used as inputs for the model domain boundary corresponding with the land surface. Observation points were added to the model domain at the location of each of the transducers deployed in both sand points.

Model Calibration—Dakota Sandstone and Burro Canyon Formation (Kdb)

Canal stage and the water level in Kdb_well1 rose quickly in response to inflow from diversions on April 2. The water levels recorded in Kdb_well1 displayed a high degree of synchrony from April 2 to April 21; after this time, the water level measured in Kdb_well1 had dropped below the level of the transducer (fig. 9). Increases in water levels were only measured during sustained higher flows in the canal. Based on measured water levels, subsurface flow appeared not to reach Kdb_well2. Canal-water temperature varied from 6 to 26 °C, and measured diurnal variations were as large as 7 °C during periods of diversion. The largest diurnal variations occurred during lower canal stages. Subsurface temperatures measured in Kdb_well1 and Kdb_well2 generally increased throughout the period of record and generally reflected changes in canal water and surface temperatures (fig. 9).

Hydraulic properties of site Kdb were estimated with a VS2DH model calibrated using field data and published literature. The lack of instrumentation that could provide a deeper depth of investigation precluded the use of a VS2DH model to estimate hydraulic properties for the underlying sandstone. As such, hydraulic properties were estimated from a variety of published sources and used as inputs to model simulations. Model inputs and data sources are listed in table 5. A hydraulic conductivity of 5×10^{-6} m/s for the silty clay was estimated using a calibrated VS2DH model and agrees with published values (Meyer and others, 1997). The sandstone layer of



NOT TO SCALE

Figure 7. Generalized installation diagram for site Kdb.

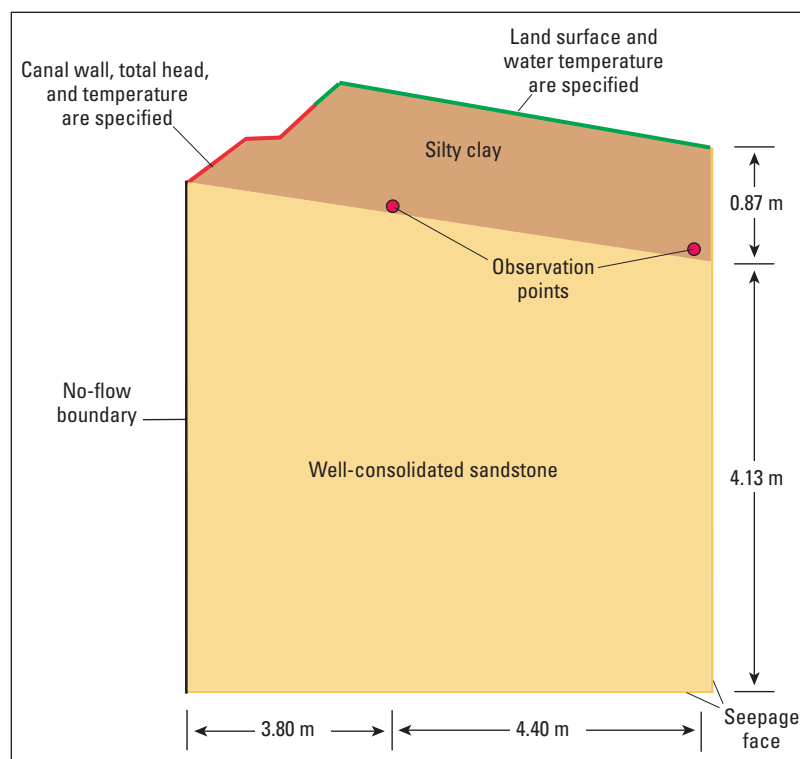


Figure 8. Generalized two-dimensional VS2DH model for site Kdb. (m, meter)

the model assumed spatially constant hydraulic conductivity and was calibrated to 1×10^{-8} m/s. This value conformed to published values (Freeze and Cherry, 1979) that accounted for flow through fractured sandstones.

Based on the modeling results of the Mancos Shale site (Km) and the Dakota Sandstone and Burro Canyon Formation site (Kdb), the shale site appears to have a higher hydraulic conductivity than the sandstone site. This outcome is counterintuitive, as the sandstone should have a higher hydraulic conductivity than the shale. These modeled results could be attributed to extensive weathering and fracturing in the shale, which could increase the amount of available flow paths and increase the hydraulic conductivity higher than published values for shale.

Salinity Loads from Agricultural Land

On-farm salinity load estimates (tail water plus deep percolation) were characterized for each irrigated subbasin in the study area. Tail water is the surface runoff resulting from irrigation practices. Deep percolation is the water that drains down past the effective root depth as a result of irrigation practices. Tail water and deep percolation are both considered in the water balance within this report, with tail water comprising a surface-water component and deep percolation comprising a groundwater component. Tail water and deep percolation flow rates and concentrations were not measured directly during the study period, so tail-water salinity loads and deep percolation salinity loads were estimated.

Tail-Water Salinity Loads

Tail-water salinity loads were estimated in each irrigated subbasin. The tail-water volume was estimated by solving for Q_{SW} using equation 2. This volume of water was assumed to be the tail water and rainfall/snowmelt runoff component. Because tail-water TDS was not measured during the study period, it was assumed the TDS of the tail water was equal to the average-flow-weighted TDS of the canal water.

Deep Percolation Salinity Loads

Deep percolation volume in each subbasin was determined by a ratio of the canal seepage volume to the total infiltrated water volume. Total infiltrated water volume was estimated by subtracting the aforementioned tail-water volume estimate from a known farm delivery volume. The known farm delivery volume was assumed to be the maximum amount of water needed to allow a crop to grow at maximum capacity and maximum consumptive use (Allen and others, 1998). The developed ratio was used to parse out the groundwater volume into agricultural components (seepage and deep percolation) of the water budget. The ratios used for each subbasin can be found in table 6. Salinity loads for groundwater were then calculated by multiplying base-flow TDS concentration by annual seepage and deep percolation water volumes and a conversion factor to obtain units of tons per year. A portion of natural water volume is contained in the groundwater and tail-water volume estimates and is not estimated in this study. Natural salinity load was estimated using field data, however, and was adjusted for in the final salinity budget.

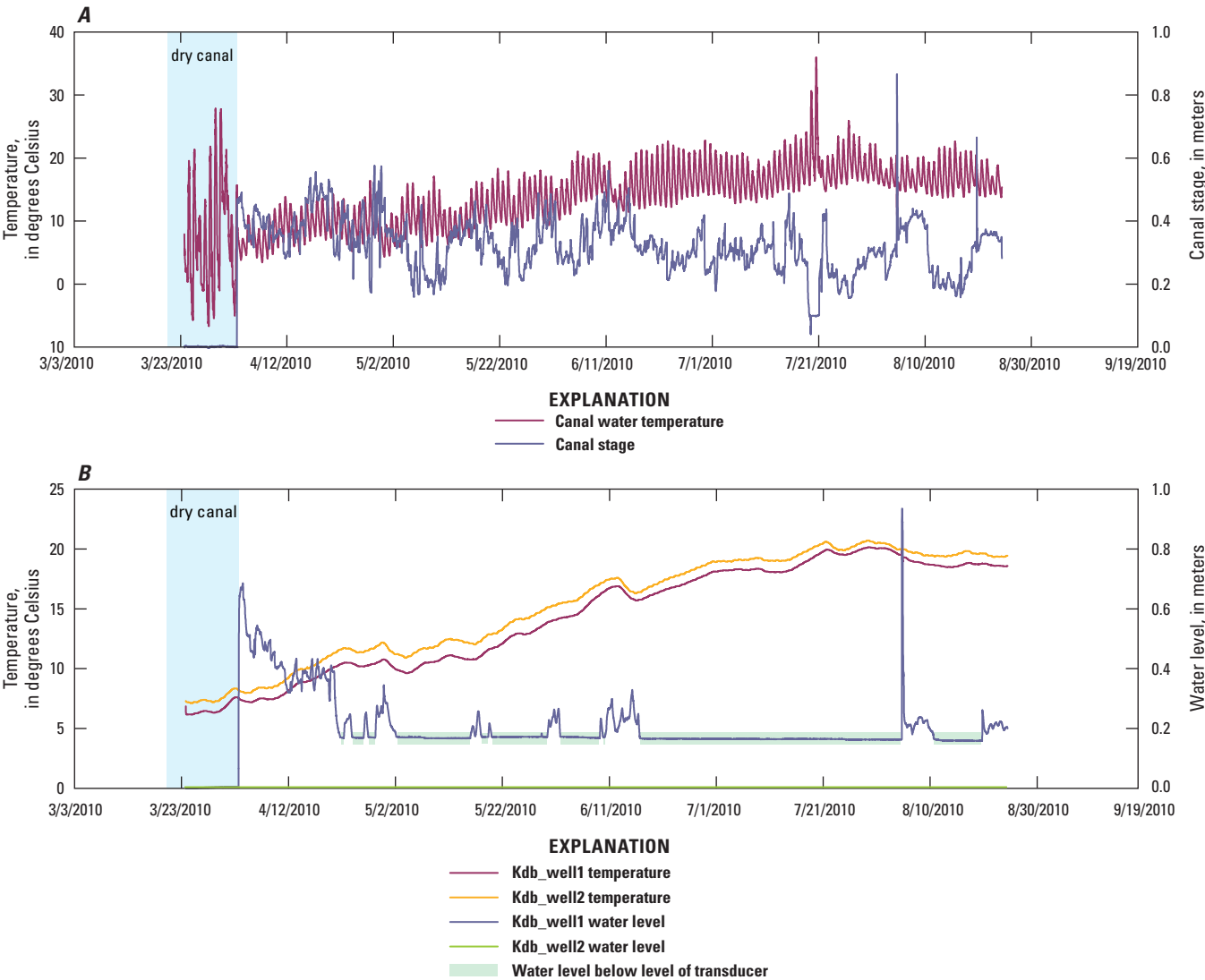


Figure 9. Observed temperature, canal stage, and water level data for site Kdb. *A*, Canal water temperature and stage. *B*, Temperature and water level for Kdb_well1 and Kdb_well2.

Natural Salinity Load Estimation

The natural salinity load for each subbasin was estimated using the salinity yield (load per acre) for different geologies. The four natural water-quality monitoring sites in the study basin were used to develop the salinity yield for the study period for each geologic setting. Sites RCG1 and RCG2 were used to estimate a salinity yield for the Dakota Sandstone and Burro Canyon Formation, site BkKm was used to estimate a yield for the Mancos Shale, and site SF1 was used to estimate a yield for the crystalline igneous and metamorphic rocks of the West Elk Mountains. The total salinity load estimated at each of the natural water-quality monitoring sites was divided by the number of acres in the subbasin to estimate the salinity yield (load per acre). The natural salinity yield for each geology type was then applied to the respective number of acres in the other subbasins to estimate a total natural salinity load. All natural salinity yields were based on the estimated salinity loads for the study period, April 2008–March 2009.

Nonagricultural Salinity Load Estimation

Nonagricultural salinity load is any salinity load that is neither related to agricultural practices nor considered part of the natural salinity load. Industrial practices and municipal use are typically the largest contributors to the nonagricultural salinity load. In a rural setting it is difficult to distinguish exactly how the water is being used and who is actually using it. Therefore, for the purposes of this study, municipal use is the only form of nonagricultural practice in the study basin.

Crawford, Colo., is the only municipality that is completely within the study boundaries. Calculation of the salinity load for Crawford was based on water usage estimated from the total population of Crawford (U.S. Census Bureau, 2009) and an estimation of the average urban-water consumption in Colorado (Waskom and Neibauer, 2006). To estimate the load, a concentration of 1,444 milligrams per liter (mg/L) was used based on the loading factor estimated for subbasin SF2 (table 4).

The estimated volume of consumption and concentration were multiplied by the conversion factor 0.0027 to calculate the annual salinity load generated from municipal use.

Selenium Load Estimation

Surface-water selenium loads were estimated for each subbasin using a ratio of selenium concentration to salinity (TDS) concentration of the six periodic samples collected at each sampling location (table 7). The selenium concentration to salinity concentration ratio was applied to each 15-minute interval. Each continuous (15 minute) salinity value was multiplied by the Se/salinity ratio to calculate a continuous selenium time series. Selenium loads were then estimated by using the following equation:

$$L = Q_{efs} \times C \times 0.000056197 \quad (7)$$

where

L is the selenium load, in pounds per 15 minutes;
 Q_{efs} is the streamflow, in cubic feet per second;
 C is the selenium concentration, in microgram per liter; and

0.000056197 is the conversion factor to convert to pounds per 15 minutes.

Surface-water selenium loads calculated for each 15-minute interval were summed for the study period to represent an annual surface-water selenium load in pounds.

All attempts to estimate the groundwater selenium load resulted in selenium loads that exceeded observed selenium loads at downstream monitoring sites on the Gunnison River. The Gunnison River monitoring sites were assumed to have integrated all basin surface water and groundwater; therefore, the total selenium loads for the study area should fit reasonably within the selenium loads measured in the Gunnison River monitoring sites. However, estimated groundwater

selenium loads in the study area exceeded observed selenium loads measured at the Gunnison River monitoring sites. The difference between estimated groundwater selenium loads in the study area and observed selenium loads at Gunnison River monitoring sites may be a result of geochemical processes in the subsurface that were beyond the scope of this study. Because a reasonable estimate of groundwater selenium was not able to be completed, there is no estimated groundwater selenium load reported in this report.

Error Analysis

To determine the compound effects of salinity load calculations from equation 5, an error analysis was performed for each sampling location using error-propagation techniques (Taylor, 1997). Error can be introduced through field methods (sampling, processing, and shipping) and analytical methods (processing and data analysis).

Streamflow-measurement error was calculated with FlowTracker software for each streamflow measurement. FlowTracker uses a USGS certified method for streamflow-measurement error (SonTek/YSI Inc., 2007). The streamflow measurement error was averaged for the six streamflow measurements for each site. Regression analysis was used to estimate streamflow based on gage height and measured streamflow from the six measurements. Error associated with the regression model used to determine the rating curve was estimated from the standard error of prediction (Helsel and Hirsch, 2002). The standard error of prediction was compared to the predicted value for each 15-minute interval, and a percent error was estimated for each 15-minute streamflow value. A flow-weighted average percent error was calculated from the 15-minute intervals and then added to the estimated error of the streamflow measurements.

Error associated with the TDS concentration used in equation 5 was estimated based on laboratory analysis error and regression error. Laboratory analysis error was estimated by

Table 6. Ratios used to separate canal seepage and deep percolation from drain base flow (in total dissolved solids) for selected sites in the study area.

[AL1, Alum Gulch; B1, Bell Creek; BkKm, North Fork Gunnison River tributary (background Mancos Shale site); CK1, Cottonwood Creek; R1, Reynolds Creek; SF1, Smith Fork Creek near Crawford, CO; SF2, Smith Fork Creek at 38.5 Road bridge near Hotchkiss, CO; SF3, Smith Fork Creek above mouth near Black Canyon; RCG1, Red Canyon at Poison Springs Gulch; RCG2, Red Canyon near Trail Gulch; --, no data available]

	AL1	B1	BkKm	CK1	R1	RCG1	RCG2	SF1	SF2	SF3
Canal seepage ratio	0.25	0.30	--	0.42	0.44	--	--	--	0.15	0.34
Deep percolation ratio	0.75	0.70	--	0.58	0.56	--	--	--	0.85	0.66

Table 7. Summary of ratios of surface-water selenium concentration (in micrograms per liter) to salinity concentration (in milligrams per liter) at selected sites in the study area.

[AL1, Alum Gulch; B1, Bell Creek; BkKm, North Fork Gunnison River tributary (background Mancos Shale site); CK1, Cottonwood Creek; R1, Reynolds Creek; SF1, Smith Fork Creek near Crawford, CO; SF2, Smith Fork Creek at 38.5 Road bridge near Hotchkiss, CO; SF3, Smith Fork Creek above mouth near Black Canyon; RCG1, Red Canyon at Poison Springs Gulch; RCG2, Red Canyon near Trail Gulch; --, no data available]

	AL1	B1	BkKm	CK1	R1	RCG1	RCG2	SF1	SF2	SF3
Selenium concentration to salinity concentration ratio	0.000823	0.00420	--	0.00413	0.00674	0.00535	0.00538	0.00358	0.00116	0.00167

calculating the percent difference between the environmental sample, replicates, and rerun values and the mean value of the environmental, replicates, and rerun values. The percent difference of the environmental sample to the mean, the replicate to the mean, and the rerun to the mean were averaged to result in an average percent error. Error associated with the regression analysis was estimated for the relation between TDS and specific conductance by using the same process as the streamflow regression error analysis. Assessing the error associated with the water balance exercise required an understanding of the error associated with the PRISM predictions and the error associated with the estimation of ET using the Penman-Monteith method. Canal flow estimation also had an associated error. The percent error associated with PRISM predictions was determined using findings in Jeton and others (2005). They compared precipitation estimates from PRISM in the state of Nevada with reported precipitation values from the National Weather Service (NWS) from 1971 to 2000. Their finding indicated that the percent difference between PRISM and NWS data ranged from 5 to 15 percent. Based on these findings, the percent error for the PRISM estimations in this study was 10 percent, which was the average of the difference found in Jeton and others (2005). Error associated with ET predictions using the Penman-Monteith method were determined using results from Howell and Evett (2004). Howell and Evett compared predictions using the Penman-Monteith ET method with measured values of ET. Results indicated that predictions had less than 5 percent difference from measured values. Using these results, a percent error of 5 percent was chosen for the purposes of this study. Estimations of canal flows were given an error of 15 percent, which is considered a reasonable estimate associated with a fair indirect measurement possible error (Benson and Dalrymple, 1967). A fair indirect measurement represents an estimation having neither natural conditions nor favorable field data. Field estimations of canal flow were determined to be better than a poor estimation (error of 25 percent or greater) but not within the criteria of a good estimation (error of 10 percent) as described by Benson and Dalrymple (1967).

Salinity Load Error Analysis

The error inherent in salinity load calculations was quantified using error analysis techniques. Rules for error analysis described in Taylor (1997) were used to estimate the error associated with the salinity load calculation. The calculation of the salinity load error is based on the following equation:

$$L_{error} = Q_{error} + C_{error} \quad (8)$$

where

- L_{error} is the total error associated with salinity load calculation, in percent;
- Q_{error} is the error associated with streamflow estimates, in percent; and
- C_{error} is the error associated with TDS concentration estimates, in percent.

Selenium Load Error Analysis

The error inherent with selenium load calculations was quantified by using an error analysis. Error associated with the 15-minute streamflow estimations were determined as previously described. Selenium concentration error for each 15-minute interval was calculated from error associated with field and analytical methods. The calculating of the total uncertainty of the 15-minute selenium concentration error was based on the general formula of error propagation in Taylor (1997), expressed in the following equation:

$$\delta Se_{15} = \sqrt{\left(\frac{\partial Se_{15}}{\partial Se_p} \delta Se_p\right)^2 + \left(\frac{\partial Se_{15}}{\partial TDS_{15}} \delta TDS_{15}\right)^2 + \left(\frac{\partial Se_{15}}{\partial TDS_p} \delta TDS_p\right)^2} \quad (9)$$

where

- δSe_{15} is the total uncertainty associated with each 15-minute selenium concentration prediction, in micrograms per liter;
- $\frac{\partial Se_{15}}{\partial Se_p}$ is the partial derivative of each 15-minute selenium concentration, in micrograms per liter, with respect to periodic selenium sample concentration, in micrograms per liter;
- δSe_p is the standard deviation associated with the periodic selenium sample concentrations, in micrograms per liter;
- $\frac{\partial Se_{15}}{\partial TDS_{15}}$ is the partial derivative of each 15-minute selenium concentration, in micrograms per liter, with respect to the 15-minute total dissolved solids concentration, in milligrams per liter;
- δTDS_{15} is the standard deviation associated with the 15-minute total dissolved solids concentration, in milligrams per liter;
- $\frac{\partial Se_{15}}{\partial TDS_p}$ is the partial derivative of each 15-minute selenium concentration, in micrograms per liter, with respect to the periodic total dissolved solids concentration, in milligrams per liter; and
- δTDS_p is the standard deviation associated with the periodic total dissolved solids concentration, in milligrams per liter.

The total error associated with the selenium load estimations were calculated using equation 5 and replacing TDS concentration with selenium concentration.

Error analysis is an indicator of the accuracy of the estimated salinity load/selenium load calculations. The percent error associated with salinity load/selenium load estimations was used to estimate the total annual salinity load/selenium load error in tons per pound. The error-analysis estimations provide a range of salinity load/selenium load values and are represented by error bars.

Characterization of Salinity Loads and Selenium Loads

Salinity and selenium loads were calculated for each subbasin for the study period April 2008–March 2009. Salinity and selenium load calculations differed in how they were quantified. For selenium, only surface-water load at the gage site was calculated because of the complexities associated with the nonconservative nature of selenium in groundwater. Salinity, however, is widely accepted as being a conservative measure of water quality and therefore both the surface-water and groundwater components of load were estimated.

Water Budget

A water balance was used to estimate the groundwater component of each subbasin. Results of the water balance indicate there is a considerable groundwater discharge in many of the subbasins (table 8). Subbasins that are affected by agricultural practices tended to have a larger groundwater component than many of the natural subbasins in the study area. Groundwater volumes ranged from 0 to 47,200 acre-ft. Subbasins SF2 and SF3 had the largest volume of groundwater for the study period with 47,200 acre-ft and 18,000 acre-ft, respectively. Subbasins BkKm and SF1 had groundwater volumes of 0 acre-ft. This result for subbasin SF1 might be inaccurate; the water balance equation indicated a groundwater volume of –23,400 acre-ft. Because the volume of outgoing water is much greater than the volume of incoming water, it is believed that an unknown input existed, presumably a groundwater input to the subbasin.

Adjacent basins that share headwaters with subbasin SF1 and are similar in size and precipitation amounts tend to have smaller surface-water flow volumes. Minnesota Creek is a 26,400-acre basin that is monitored by USGS stream gage 09134000 Minnesota Creek near Paonia, CO. The 2009 Annual Data Report indicated that the annual flow for

water year 2009 was 16,000 acre-ft (U.S. Geological Survey, 2009). Subbasin SF1 contains 27,000 acres, and monitored streamflow at the SF1 gage was 47,000 acre-ft. The difference between the two subbasins may indicate that precipitation in the Minnesota Creek watershed may manifest in subbasin SF1. A similar relation is seen between subbasin SF1 and the headwaters of Coal Creek, which is the watershed adjacent to SF1 to the east. Because Coal Creek is an ungaged watershed, the USGS Colorado StreamStats program was used to get an average streamflow for the watershed based on regression analysis (U.S. Geological Survey, 2011). After delineating the Coal Creek watershed to the confluence with Little Robinson Creek (watershed area of 17,300 acres), the results from StreamStats showed an average annual flow of 18,700 acre-ft. Streamflow in this watershed is also less than what was gaged in subbasin SF1 and may also indicate water moving transbasinally into subbasin SF1. Therefore, quantifying groundwater volumes by the water balance approach might not have worked effectively in subbasin SF1 because an unidentified water input may have been missing from the water balance equation.

Each agricultural subbasin was separated into on-farm and off-farm water volumes. As mentioned previously, the on-farm component is also referred to as deep percolation from applied irrigation, and the off-farm component is also referred to as seepage from the irrigation delivery system (canals).

A calibrated VS2DH model was used to model seepage rates from the canals. The boundary flux extension to VS2DH was used to calculate the daily seepage rate. The model generated a daily canal seepage rate for each monitoring well location. Canal seepage at site Km remained relatively constant throughout the monitoring period, with daily seepage rates ranging between 0.12 and 0.19 meters per day (m/d) (table 9). The average daily seepage rate at site Km for the observation period was 0.14 m/d (fig. 10; table 9).

The boundary flux extension to VS2DH was used to calculate the daily seepage at site Kdb, similar to the method used in the Km model. The period simulated at site Kdb began when the canal was dry; consequently, the transition

Table 8. Summary of water budget allocations (in acre-feet) at selected sites in the study area, April 2008–March 2009.

[AL1, Alum Gulch; B1, Bell Creek; BkKm, North Fork Gunnison River tributary (background Mancos Shale site); CK1, Cottonwood Creek; R1, Reynolds Creek; SF1, Smith Fork Creek near Crawford, CO; SF2, Smith Fork Creek at 38.5 Road bridge near Hotchkiss, CO; SF3, Smith Fork Creek above mouth near Black Canyon; RCG1, Red Canyon at Poison Springs Gulch; RCG2, Red Canyon near Trail Gulch]

	AL1	B1	BkKm	CK1	R1	RCG1	RCG2	SF1	SF2	SF3
Inputs										
Precipitation	6,140	12,200	245	31,700	9,390	4,350	9,730	62,300	98,000	24,500
Canal diversions into subbasin	18,700	19,600	0	29,200	26,300	0	0	0	80,200	17,900
Tributary inflow	0	0	0	0	0	0	0	0	47,000	27,100
Outputs										
Gaged streamflow	5,910	4,280	1.7	6,600	695	90.9	2.86	47,000	27,100	29,200
Ungaged groundwater	8,440	12,600	0	17,800	5,990	290	1700	0	47,200	18,000
Canal diversions out of subbasin	627	1,870	0	6,130	19,600	0	0	4,650	53,600	377
Crop consumptive use	8,580	6,200	0	9,830	3,630	0	0	0	17,100	11,300
Other consumptive use ¹	5,610	9,990	201	25,600	6,240	3,970	8,060	34,000	82,700	14,700

¹Other consumptive use includes natural consumptive use, reservoir evaporation, and phreatophyte consumptive use.

from unsaturated to saturated conditions was observed. The maximum seepage during unsaturated conditions was 11.3 m/d (table 9). Canal seepage for the first nine days of observation averaged 3.89 m/d; once saturated, however, the seepage averaged 0.02 m/d (fig. 11). On July 19, 2010, the water level in the canal was low enough that the canal gained groundwater from the banks.

Salinity Loads

Salinity loads in the study area vary widely from sub-basin to subbasin. All the studied subbasins contain a natural salinity load, and subbasins with agriculture practices contain an agricultural salinity load.

Natural Salinity Load

The natural salinity load for each subbasin is based on the salinity load totals of the four natural subbasins. Sites RCG1 and RCG2 represented the Dakota Sandstone and Burro Canyon Formation geology, site BkKm represented the Mancos Shale geology, and site SF1 represented the Tertiary crystalline volcanics of the West Elk Mountains.

Applying the appropriate salinity yield to the number of corresponding acres resulted in the natural salinity load component for each subbasin. The salinity yields for the Dakota Sandstone and Burro Canyon Formation, Mancos Shale, and crystalline geologies are 0.217 tons per acre (t/acre), 0.113 t/acre, and 0.151 t/acre, respectively.

It is important to mention that the natural salinity loads were calculated based on measured salinity loads only for the study period April 2008–March 2009. Therefore, natural salinity loads and yields are based on the amount of natural precipitation that was captured during the study period. For instance, site BkKm experienced one precipitation event in August 2008 that totaled an estimated 71.7 acre-ft of discharge and a corresponding load of 27.9 tons (t). There was no runoff from snowmelt at the site in the spring of 2009. As a result, the natural salinity yield of the Mancos Shale was based on the one convective storm event. A similar situation was observed at subbasin RCG2, representing the Dakota Sandstone and Burro Canyon Formation. At site RCG2, a small amount of snowmelt was observed during the spring of 2008 totaling 1,700 acre-ft and a salinity load of 2,180 t. There

Table 9. Summary of seepage rates (in meters per day) calculated using the boundary flux extension of the VS2DH model at sites Km and Kdb.

	Mancos Shale, Km	Dakota Sandstone and Burro Canyon Formation, Kdb
Minimum seepage rate	0.12	0.003
Maximum seepage rate	0.19	11.3
Average seepage rate	0.14	0.02

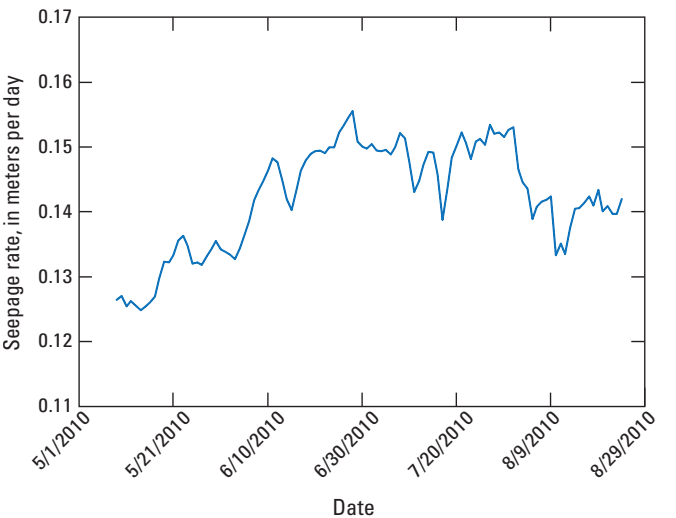


Figure 10. Calculated daily seepage rate (in meters per day), using the boundary flux extension of VS2DH at site Km.

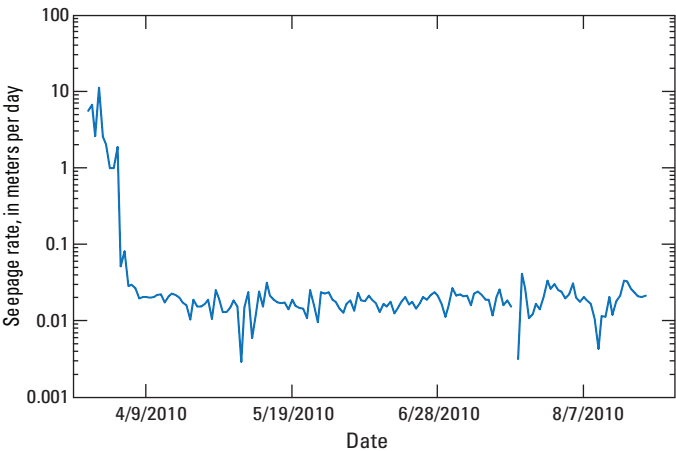


Figure 11. Calculated daily seepage rate (in meters per day), using the boundary flux extension of VS2DH at site Kdb.

were no recorded flows from storm events at the monitor and no snowmelt observed during the spring of 2009 at the site. However, even though the numbers of events are limited in these subbasins during the study period, they are believed to be representative of the natural condition that occurred during April 2008–March 2009.

Based on the calculated natural salinity yields for the various geological types, the natural salinity load for each subbasin was calculated based on the number of acres of Dakota Sandstone and Burro Canyon Formation, Mancos Shale, and crystalline rock in each subbasin. The four natural subbasins—RCG1, RCG2, SF1, and BkKm—had salinity loads of 371 tons per year (t/yr), 2,180 t/yr, 3,730 t/yr, and 27.9 t/yr, respectively. The remaining six agriculturally influenced subbasins—AL1, B1, CK1, R1, SF2, and SF3—had natural salinity loads of 1,040 t/yr, 1,020 t/yr, 3,040 t/yr, 740 t/yr, 9,490 t/yr, and 4,570 t/yr, respectively.

Agricultural Salinity Load

Agricultural salinity loads were calculated for subbasins that had agricultural practices. The agricultural salinity load was separated into three components: tail water, deep percolation, and canal seepage. The tail-water salinity load was generally the smallest component compared to deep percolation and canal seepage.

Tail-water salinity loads ranged from 48.0 t/yr to 2,750 t/yr in the study area. The largest tail-water salinity load was in subbasin SF3, and the lowest salinity load from tail water was in subbasin R1. The remaining four agricultural subbasins—AL1, B1, CK1, and SF2—had tail-water loads of 285 t/yr, 180 t/yr, 333 t/yr, and 1,700 t/yr, respectively (table 10).

The deep percolation component of the agricultural salinity load ranged from 3,300 t/yr in subbasin AL1 to 51,800 t/yr in subbasin SF2. Subbasins R1, B1, CK1, and SF3 had deep percolation salinity loads of 4,940 t/yr, 15,200 t/yr, 21,200 t/yr, and 23,600 t/yr, respectively (table 10). Typical deep percolation salinity loads were in the range of 55 to 85 percent of the total agricultural salinity load for each subbasin.

The canal seepage component of the agricultural salinity component ranged from 1,100 t/yr in subbasin AL1 to 15,300 t/yr in subbasin CK1. Subbasins B1, R1, SF2, and SF3 had canal seepage salinity loads of 6,610 t/yr, 3,890 t/yr,

9,430 t/yr, and 12,100 t/yr, respectively (table 10). Canal seepage salinity load were generally in the range of 15 to 45 percent of the total agricultural salinity load.

Total Salinity Load

Total salinity loads at each site were a combination of measured surface-water salinity loads and estimated groundwater salinity loads. The total salinity load was divided into three components: natural salinity load, municipal salinity load, and agricultural salinity load. Total salinity loads were adjusted to take incoming or outgoing canal salinity load into effect.

Instantaneous data collected at each of the 10 continuous monitors were summed on a monthly basis and then summed to an annual value for April 2008–March 2009. The highest salinity loading months tended to be May and June, which correspond with higher streamflows from snowmelt and spring precipitation events. The highest estimated monthly salinity loads during the study period were at sites SF3, SF2, and CK1 (table 11). Site SF3 had the highest salinity loads during the months of April, May, and June with estimated salinity loads of 2,720 t, 5,920 t, and 2,950 t, respectively. Site SF2 appeared to have a runoff period a little later and had its highest salinity loads during months May and June, with salinity loads of

Table 10. Summary of annual agricultural salinity loads (in tons) at selected sites in the study area, April 2008–March 2009.

[AL1, Alum Gulch; B1, Bell Creek; BkKm, North Fork Gunnison River tributary (background Mancos Shale site); CK1, Cottonwood Creek; R1, Reynolds Creek; SF1, Smith Fork Creek near Crawford, CO; SF2, Smith Fork Creek at 38.5 Road bridge near Hotchkiss, CO; SF3, Smith Fork Creek above mouth near Black Canyon; RCG1, Red Canyon at Poison Springs Gulch; RCG2, Red Canyon near Trail Gulch; n.a., not applicable]

	AL1	B1	BkKm	CK1	R1	RCG1	RCG2	SF1	SF2	SF3
Agricultural salinity load ¹	4,680	22,000	n.a.	36,800	8,880	n.a.	n.a.	n.a.	62,900	38,400
Tail-water salinity load	285	180	n.a.	333	48	n.a.	n.a.	n.a.	1,700	2,750
Deep percolation salinity load	3,300	15,200	n.a.	21,200	4,940	n.a.	n.a.	n.a.	51,800	23,600
Canal seepage salinity load	1,100	6,610	n.a.	15,300	3,890	n.a.	n.a.	n.a.	9,430	12,100

¹Values adjusted (decreased) by 19.4 percent (as seen in table 12) because of wet conditions in 2008 and 2009 relative to long-term record at USGS streamflow-gaging station 09152500, Gunnison River near Grand Junction, CO.

Table 11. Estimated monthly gaged-salinity loads (in tons) at selected sites in the study area, April 2008–March 2009.

[AL1, Alum Gulch; B1, Bell Creek; BkKm, North Fork Gunnison River tributary (background Mancos Shale site); CK1, Cottonwood Creek; R1, Reynolds Creek; SF1, Smith Fork Creek near Crawford, CO; SF2, Smith Fork Creek at 38.5 Road bridge near Hotchkiss, CO; SF3, Smith Fork Creek above mouth near Black Canyon; RCG1, Red Canyon at Poison Springs Gulch; RCG2, Red Canyon near Trail Gulch; --, no data available]

Month	AL1	B1	BkKm	CK1	R1	RCG1	RCG2	SF1	SF2	SF3
April 2008	985	676	--	1,820	126	--	--	397	629	2,720
May 2008	1,310	733	--	2,070	102	9.87	0.285	1,850	2,910	5,920
June 2008	1,570	951	--	1,740	99.3	--	--	808	2,500	2,950
July 2008	1,050	645	--	1,290	72.4	--	--	165	445	815
August 2008	567	584	27.9	1,570	88.4	--	--	62.0	124	13.1
September 2008	675	639	--	1,160	56.7	--	--	28.3	108	65.7
October 2008	803	476	--	1,300	40.0	--	--	51.0	106	212
November 2008	872	419	--	1,410	144	--	--	49.9	144	762
December 2008	919	737	--	1,140	145	--	--	56.7	133	857
January 2009	791	1,150	--	1,200	137	--	--	65.3	119	721
February 2009	558	844	--	892	95.5	--	--	71.7	106	825
March 2009	712	411	--	732	55.1	--	--	126	121	1,020
Annual salinity load	10,800	8,270	27.9	16,300	1,160	9.87	0.285	3,730	7,440	16,900

2,910 t and 2,500 t, respectively (table 11). The majority of the agriculturally influenced subbasins—AL1, B1, CK1, R1, SF2, and SF3—had relatively constant salinity loads throughout the study period. Most sites maintained a higher salinity load during the spring months which then decreased during the main irrigation summer months. The base-flow period during the winter months tended to be steady at each site from month to month. The lowest salinity loading months were September and October. Smith Fork Creek experienced reduced salinity loads during these months as a result of reduced flows. Site SF3 had a salinity load of 13.1 t in the month of August, a result of very low to no streamflow reaching the monitoring site during August. August and September were also low salinity loading months for the headwaters of Smith Fork Creek. Site SF1 had its two lowest salinity loading months in September and November with salinity loads of 28.3 t and 49.9 t, respectively (table 11). The middle site on Smith Fork Creek (SF2) remained fairly constant during these months with salinity loads of 124 t and 108 t for August and September, respectively. The higher salinity loads estimated at site SF2 could be a result of reservoir water supplementation from Crawford Reservoir used for irrigation in subbasins SF2 and SF3.

Annual gaged-salinity loads ranged from 0.285 t/yr to 16,900 t/yr. Typically, the four natural subbasins had lower gaged-salinity loads than subbasins that were influenced by agriculture. The four natural subbasins—SF1, RCG1, RCG2, and BkKm—had annual gaged-salinity loads of 3,730 t/yr, 9.87 t/yr, 0.285 t/yr, and 27.9 t/yr, respectively (table 11). The six agriculturally influenced subbasins—AL1, B1, CK1, R1, SF2, and SF3—had annual gaged-salinity loads of 10,800 t/yr, 8,270 t/yr, 16,300 t/yr, 1,160 t/yr, 7,440 t/yr, and 16,900 t/yr, respectively (table 11).

Groundwater salinity loads were estimated for each subbasin by using the water balance approach discussed in the “Data Collection and Analysis” section of this report (p. 4) and the concentrations reported in table 4. Groundwater

salinity loads ranged from 0 to 92,700 t/yr (table 12). The four natural subbasins had low groundwater salinity loads which correspond with the low groundwater volumes reported in table 8. Two of the four natural subbasins, BkKm and SF1, had groundwater salinity loads of 0 t/yr for the study period. Subbasins RCG1 and RCG2 had groundwater salinity loads of 361 t/yr and 2,180 t/yr, respectively (table 12). The remaining subbasins—AL1, B1, CK1, R1, SF2, and SF3—had groundwater salinity loads of 18,700 t/yr, 32,100 t/yr, 56,000 t/yr, 13,900 t/yr, 92,700 t/yr, and 55,500 t/yr, respectively.

Total salinity loads for each subbasin were calculated by summing the tail-water salinity load and the estimated groundwater salinity load (seepage plus deep percolation), then subtracting or adding the appropriate canal salinity loads to each subbasin (table 12). Removing the incoming salinity load from several subbasins greatly reduced the total load estimated for the basin. For example, at site AL1, total annual salinity load decreased from approximately 19,900 t to 6,020 t after incoming salinity load from canal diversions was accounted for.

Errors for annual estimations were included with the annual total to indicate the possible range of the estimated annual value based on the methodologies used. A summary of error analysis for each subbasin is listed in table 13. Total salinity loads ranged from 27.9 ± 19.1 t/yr to $87,500 \pm 80,500$ t/yr. The four natural subbasins—BkKm, RCG1, RCG2, and SF1—had total salinity loads of 27.9 ± 19.1 t/yr, 371 ± 248 t/yr, $2,180 \pm 1,590$ t/yr, and $4,200 \pm 2,720$ t/yr, respectively (fig. 12).

The agriculturally influenced sites have salinity loads that range from $7,580 \pm 6,900$ t/yr to $87,500 \pm 80,500$ t/yr. Subbasin R1 had the highest error in salinity load estimation at 376 percent. Because the error is more than 100 percent and salinity load estimations cannot be a negative number, the range of salinity load estimation could range from 0 to 44,500 t/yr. The annual salinity loads for subbasins AL1, B1, CK1, SF2, and SF3 were $7,580 \pm 6,900$ t/yr, $28,300 \pm 26,700$ t/yr, $48,700 \pm 36,100$ t/yr, $87,500 \pm 80,900$ t/yr, and $52,200 \pm 31,800$ t/yr, respectively (fig. 12). The high

Table 12. Summary of annual salinity loads (in tons per year) at selected sites in the study area, April 2008–March 2009.

[AL1, Alum Gulch; B1, Bell Creek; BkKm, North Fork Gunnison River tributary (background Mancos Shale site); CK1, Cottonwood Creek; R1, Reynolds Creek; SF1, Smith Fork Creek near Crawford, CO; SF2, Smith Fork Creek at 38.5 Road bridge near Hotchkiss, CO; SF3, Smith Fork Creek above mouth near Black Canyon; RCG1, Red Canyon at Poison Springs Gulch; RCG2, Red Canyon near Trail Gulch; --, no data; n.a., not applicable]

	AL1	AL1 ¹	B1	BkKm	CK1	R1	RCG1	RCG2	SF1	SF2	SF3
Groundwater load	18,700		32,100	0	56,000	13,900	361	2,180	0	92,700	55,500
Surface-water load	1,220		259	--	511	76	--	--	--	2,570	4,290
Nonagricultural load	--		--	--	--	--	--	--	--	162	--
Natural load	1,040	1,770	1,040	27.9	3,050	751	371	2,180	3,730	9,500	4,570
Canal load added back to subbasin	482		427	n.a.	2,059	6,500	n.a.	n.a.	466	5,590	377
Canal load subtracted from subbasin	14,400		4,470	n.a.	9,810	8,760	n.a.	n.a.	n.a.	13,270	7,687
Agricultural load	4,980	5,810	27,300	n.a.	45,700	11,000	n.a.	n.a.	n.a.	78,000	47,600
Total load	6,020	7,580	28,300	27.9	48,700	11,800	371	2,180	4,200	87,500	52,200
Adjusted total load ²		6,110	22,800	22.5	39,300	9,510	299	1,760	3,390	70,500	42,070
Adjusted agricultural load ²	4,010	4,680	22,000	n.a.	36,800	8,880	n.a.	n.a.	n.a.	62,900	38,400

¹Values adjusted to account for ungaged portion of subbasin, downstream of gage site to mouth of Alum Gulch.

²Values adjusted (decreased) by 19.4 percent because of wet conditions in 2008 and 2009 relative to long-term record at USGS streamflow-gaging station 09152500, Gunnison River near Grand Junction, CO.

Table 13. Summary of associated error (in percent) in the annual salinity load estimations for selected sites in the study area, April 2008–March 2009.

[AL1, Alum Gulch; B1, Bell Creek; BkKm, North Fork Gunnison River tributary (background Mancos Shale site); CK1, Cottonwood Creek; R1, Reynolds Creek; SF1, Smith Fork Creek near Crawford, CO; SF2, Smith Fork Creek at 38.5 Road bridge near Hotchkiss, CO; SF3, Smith Fork Creek above mouth near Black Canyon; RCG1, Red Canyon at Poison Springs Gulch; RCG2, Red Canyon near Trail Gulch; TDS, total dissolved solids; ET, evapotranspiration; <, less than]

	AL1	B1	BkKm	CK1	R1	RCG1	RCG2	SF1	SF2	SF3
Surface-water flow measurement error	8.9	4.1	15.0	5.4	25.4	14.6	17.0	11.3	19.1	7.3
Surface-water rating curve error	16.8	23.3	0.0	13.1	142	0.0	0.0	2.3	5.5	3.7
TDS lab analysis error	<0.5	<0.5	<0.5	<0.5	<0.5	<0.5	<0.5	<0.5	<0.5	<0.5
TDS regression prediction error	4.8	4.8	4.2	3.6	5.6	3.8	4.4	3.8	6.6	4.4
Total surface-water salinity load error	31	32	19	22	173	18	21	17	31	16
Total groundwater estimated salinity load error ²	60	62	49	52	203	48	51	47	61	45
Total salinity load error	91	94	68	74	376	67	73	65	92	61

¹Considered a fair indirect measurement (Benson and Dalrymple, 1967).

²Calculated by summing the error associated with the components of the water balance, precipitation error (10 percent), ET error (5 percent), canal discharge error (15 percent), total surface-water flow error, and total TDS error.

salinity load in subbasin CK1 is a bit of an anomaly, as other high salinity loading subbasins, such as SF2, SF3, and B1, have dense amounts of irrigated and agricultural land within them. Subbasin CK1, on the other hand, is one of the largest subbasins in the study area, though it does not have as much irrigated land. Because of this, the mechanism that is creating the high salinity is not completely understood in this subbasin.

Overall, the pattern in the Smith Fork Creek region is for higher salinity loading to occur in agriculturally dominated subbasins. Subbasins with more irrigated land on Mancos Shale also tend to have higher salinity loads than subbasins that are not in the shale or have a mix of geology types. The natural subbasins generated little salinity load during the study period. The ephemeral stream characteristics of the natural subbasins indicate that agricultural influences are important in maintaining perennial streamflow in the agriculturally dominated subbasins.

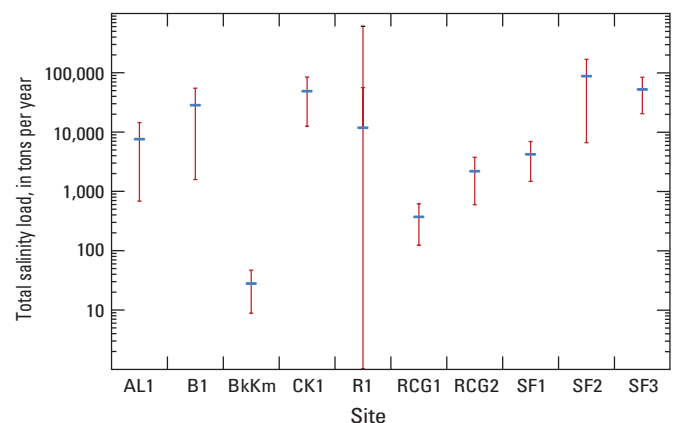
The Alum Gulch subbasin was a special case. The monitoring location for the subbasin, AL1, was located roughly halfway through the subbasin instead of near the confluence with the North Fork of the Gunnison River (fig. 13). Because the monitoring site was located halfway through the subbasin, it was necessary to estimate the remaining portion of the subbasin that was ungaged.

To estimate the ungaged salinity load associated with Alum Gulch, a yield for agricultural influenced area and natural area based on the gaged portion of the subbasin were used. The agriculturally influenced salinity yield was calculated by taking the agricultural salinity load for subbasin AL1 (4,980 t/yr; table 12) divided by the area of irrigated land use (3,833 acres). Natural salinity yield was calculated the same way, using the natural salinity load (1,040 t/yr; table 12) and natural land use area (5,173 acres). These calculations resulted in yields of 1.30 t/acre and 0.20 t/acre for irrigated land use and natural land use, respectively, for the study period. Salinity loads were calculated for the total subbasin by taking the salinity yield for natural and irrigated land use in the gaged portion and multiplying by the representative land use areas

within the total subbasin. The entire Alum Gulch subbasin area is 8,861 acres; irrigated land use accounts for 4,473 acres and natural land use accounts for 8,861 acres. The natural land use accounts for the natural salinity load from the different geologic types within the entire subbasin, whereas the irrigated land use accounts for the additional agricultural salinity load. The total salinity load calculated for the Alum Gulch subbasin is 7,580±6,900 t/yr, 5,810 t/yr from irrigated land use and 1,770 t/yr from natural land use (table 14).

Percent of Agricultural Salinity Load within the Total Salinity Load

The total loads for each subbasin were broken down into their agricultural and nonagricultural salinity load components. Excluding the four natural sites, which were all 100 percent natural load, the remaining subbasins ranged between 3 and 17 percent natural salinity load. Large subbasins with a lower percentage of irrigated land had the highest percentage of natural salinity load. The total salinity load in agriculturally effected subbasins was divided into on-farm, off-farm, and natural salinity load components.

**Figure 12.** Total salinity load (in tons per year), with error bars.

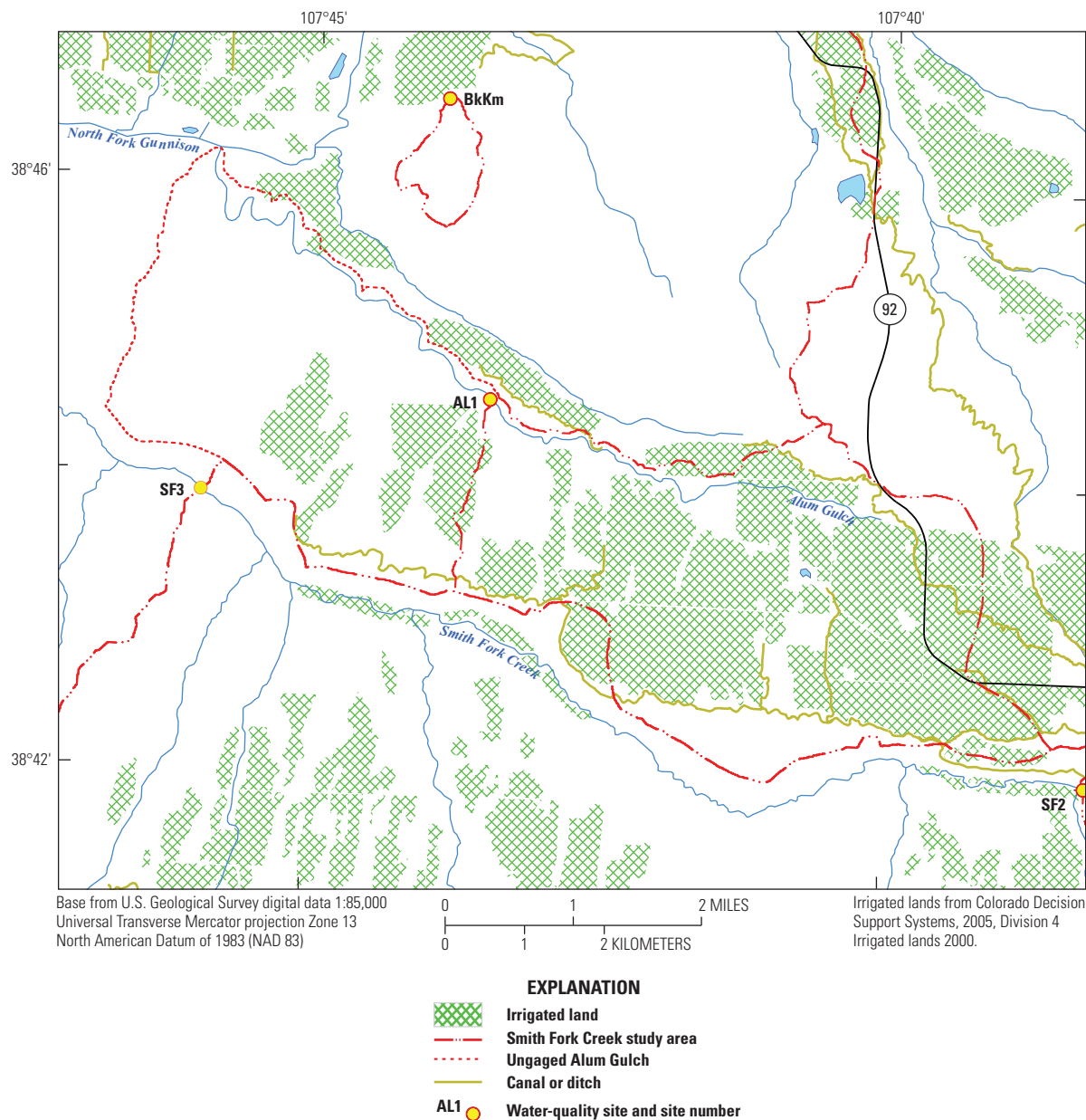


Figure 13. Location of ungaged portion of Alum Gulch in relation to site AL1.

The percent of adjusted total salinity load associated with on-farm practices ranged from 52 to 76 percent in the six subbasins. Subbasin SF2 had the highest on-farm salinity load component at 76 percent of the total salinity load. Subbasin B1 was similar to SF2 with 67 percent of the total salinity load contributed by on-farm practices. The on-farm component of the total salinity loads for the remaining subbasins—AL1, CK1, R1, and SF3—were 59 percent, 55 percent, 52 percent, and 63 percent, respectively (fig. 14).

Off-farm salinity loads for each subbasin ranged between 13 and 41 percent of the adjusted total salinity load. Subbasin SF2 had the lowest percentage of off-farm salinity load at 13 percent. The Alum Gulch subbasin and subbasins B1 and SF3 are in the middle with off-farm salinity

loads of 18 percent, 29 percent, and 29 percent of the total salinity load, respectively. Subbasins R1 and CK1 had the highest off-farm salinity loads at 41 percent and 39 percent of the total salinity load, respectively. An illustration of relative salinity load size and proportion of on-farm, off-farm, and natural salinity loads is in figure 14.

Selenium Loads

Surface-water selenium loads were calculated for each subbasin and are considered the total selenium load because ground-water selenium loads were not estimated for the study period. It was determined that the mobilization mechanisms for selenium have multiple influences, but understanding and describing

Table 14. Salinity yield and subbasin land use area used to calculate the total salinity load at the confluence of Alum Gulch and the North Fork of the Gunnison River.

Land use type	AL1 salinity yield, in tons per acre	Total area for Alum Gulch subbasin, in acres ¹	Alum Gulch salinity load, in tons per year
Natural	0.202	8,861	1,770
Irrigated	1.30	4,473	5,810

¹The area of natural land use is the same as the total area for the entire subbasin and accounts for natural salinity yield and load from the different geology types.

mobilization of selenium was outside the scope of this study. Even though it was not quantified in this study, groundwater selenium load is an important component of the total selenium load in a system and future studies may be designed to quantify the groundwater component of the selenium load.

Gaged surface-water selenium loads were estimated with an associated error for each subbasin. The subbasin designated by site CK1 had the highest selenium load with 135 ± 38.7 pounds (lb) (table 15). The next highest subbasins are B1, SF3, and SF1 with selenium loads of 69.6 ± 28.4 lb,

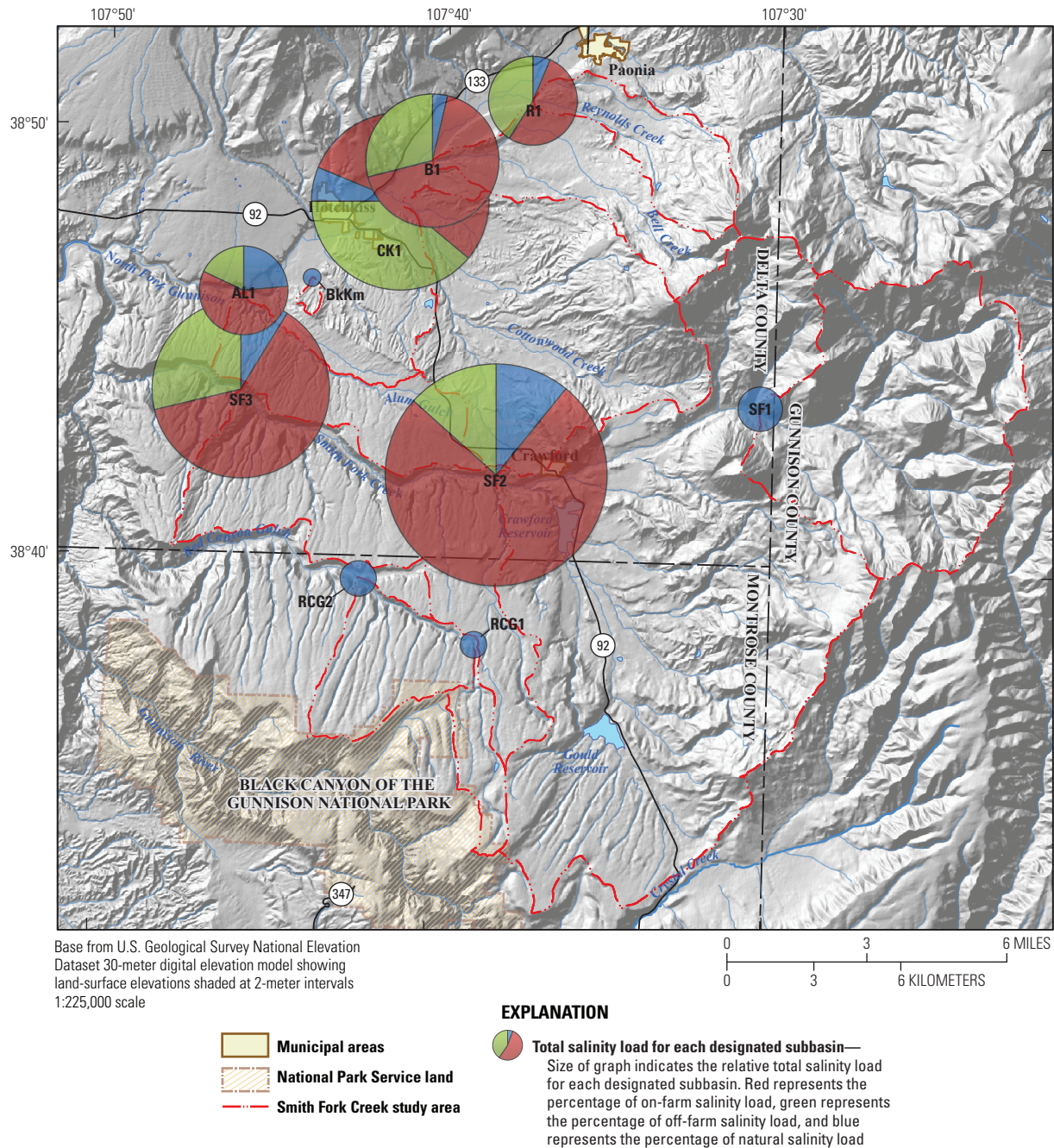


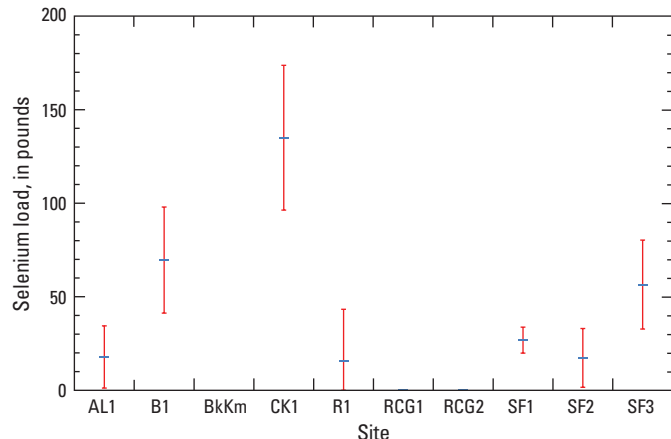
Figure 14. Relative magnitude of total salinity loads and the proportion of on-farm, off-farm, and natural salinity load for each subbasin in the study area.

Table 15. Summary of gaged selenium loads at selected sites in the study area, April 2008–March 2009.

[AL1, Alum Gulch; B1, Bell Creek; BkKm, North Fork Gunnison River tributary (background Mancos Shale site); CK1, Cottonwood Creek; R1, Reynolds Creek; SF1, Smith Fork Creek near Crawford, CO; SF2, Smith Fork Creek at 38.5 Road bridge near Hotchkiss, CO; SF3, Smith Fork Creek above mouth near Black Canyon; RCG1, Red Canyon at Poison Springs Gulch; RCG2, Red Canyon near Trail Gulch; --, no data]

	AL1	B1	BkKm	CK1	R1	RCG1	RCG2	SF1	SF2	SF3
Surface water selenium load, in pounds	17.8	69.6	--	135	15.6	0.106	0.00	26.8	17.3	56.5
Surface water selenium load error, in pounds	16.6	28.4	--	38.7	27.7	0.024	0.00	6.95	15.7	23.8
Surface water selenium load error, in percent	93.4	40.7	--	28.7	178	22.8	26.4	25.9	90.8	42.1

56.5±23.8 lb, and 26.8±6.95 lb, respectively. Subbasin R1 had a selenium load of 15.6±27.7 lb with the majority of the associated error being a result of streamflow error. Three of the four natural subbasins had little to no selenium load based on the measured data and calculated selenium loads. Subbasins RCG1 and RCG2 had surface-water selenium loads of 0.106±0.024 lb and 0.00 lb, respectively. Subbasin BkKm did not have an estimated surface-water selenium load because of the lack of any water-quality samples during the study period. Subbasin AL1, the gaged portion of the Alum Gulch subbasin (5,173 acres), had an estimated surface-water selenium load of 17.8±1.6 lb (fig. 15, table 15). To estimate the selenium load for the entire Alum Gulch subbasin (8,861 acres), the selenium yield of the gaged portion (0.00344 lb/acre) was applied to the entire basin area; the resulting selenium load for Alum Gulch is 30.5±16.6 lb.

**Figure 15.** Surface water selenium loads (in pounds), with error bars.

Summary

The lower Gunnison River Basin of the Colorado River Basin has elevated salinity and selenium levels. The Colorado River Basin Salinity Control Act of June 24, 1974 (Public Law 93–320, amended by Public Law 98–569), authorized investigation of the Lower Gunnison Basin Unit Salinity Control Project by the U.S. Department of the Interior. Salinity is generally defined as concentration of dissolved mineral salts or dissolved solids in water. Elevated salinity

concentrations can cause soil dispersion, corrosion of infrastructure for potable water supplies and irrigation delivery systems. Selenium is a trace metal that bioaccumulates in aquatic food chains and has the potential to cause deformities, and reproductive failure in birds and fish, including endangered fish species.

The Bureau of Reclamation (Reclamation) and the Natural Resources Conservation Service are responsible for assessing and implementing measures to reduce salinity and selenium loading in the Colorado River Basin. As part of this process, cost-share programs are used to involve the agricultural community in salinity reduction efforts. Cost-sharing programs help farmers, ranchers, and canal companies improve the efficiency of water delivery systems and irrigation practices. The delivery systems (irrigation canals) have been identified as potential sources of seepage, which can contribute to salinity loading. Reclamation wants to identify seepage from irrigation systems in order to maximize the effectiveness of the various salinity-control methods, such as polyacrylamide lining and piping of irrigation canal programs.

Elevated selenium concentrations in many western Colorado streams and tributaries have resulted in the placement of many streams and tributaries on the U.S. Environmental Protection Agency's 303(d) list. Identifying the potential source areas of dissolved selenium loading can provide valuable information on where improvements can be made to reduce the levels of dissolved selenium.

The Smith Fork Creek region is one of the most data-poor regions in the Lower Gunnison salinity control unit. The Smith Fork Creek region comprises seven streams—Alum Gulch, Bell Creek, Cottonwood Creek, Reynolds Creek, Red Canyon Gulch, Smith Fork Creek, and one unnamed stream. Because little is known about the potential salinity and selenium loading associated with the Smith Fork Creek region, the U.S. Geological Survey (USGS), in cooperation with Reclamation, developed a study to characterize the salinity and selenium loading there. This study will help identify where control efforts can be maximized to reduce salinity and selenium loading.

The goals of the study in the Smith Fork Creek region were to (1) characterize the total annual salinity loads for each stream subbasin, (2) characterize the groundwater component of each stream subbasin, (3) characterize the natural salinity load for each stream subbasin, (4) characterize the on-farm and off-farm salinity loads for each stream subbasin,

(5) calculate a selenium/salinity load ratio for each stream sub-basin, and (6) estimate and report the total annual salinity and selenium loads for the study period April 2008–March 2009.

The climate of the study area is semiarid to temperate with high-elevation headwaters receiving an estimated 22.5 inches of precipitation for the study period, while lower-elevation areas of the study area received an estimated 10 inches of precipitation for the study period. Long-term record at USGS streamflow-gaging station 09152500 Gunnison River near Grand Junction, CO, indicates wetter than normal conditions by approximately 19.4 percent. As a result, final agricultural and total salinity loads were reduced by 19.4 percent to better represent natural hydrologic conditions.

A water balance was used to estimate the unengaged groundwater component of each subbasin. Results of the water balance indicate there is a considerable groundwater discharge in many of the subbasins. Subbasins that are affected by agricultural practices tended to have a larger groundwater component than many of the natural subbasins in the study area. Groundwater volumes ranged from 0 to 47,200 acre-feet.

Each agricultural subbasin was separated into on-farm and off-farm water volumes. The on-farm component is also referred to as deep percolation from applied irrigation, and the off-farm component is also referred to as seepage from the irrigation delivery system. A VS2DH model was used to model seepage rates from the canals. Daily seepage rates from canals in the Mancos Shale ranged between 0.12 and 0.19 meters per day (m/d). Canals in the Dakota Sandstone and Burro Canyon Formation had a maximum seepage rate during unsaturated conditions of 11.3 m/d; once saturated, the seepage averaged 0.02 m/d.

Salinity loads in the study area vary widely from sub-basin to subbasin. All the studied subbasins contain a natural salinity load, and subbasins with agriculture practices contain an agricultural salinity load. Four natural subbasins—RCG1, RCG2, SF1, and BkKm—were used to calculate natural salinity yields for the remaining subbasins. The appropriate salinity yield was applied to the corresponding number of acres, resulting in a natural salinity load for each sub-basin. The annual salinity yields for the Dakota Sandstone and Burro Canyon Formation, Mancos Shale, and crystalline geologies are 0.217 tons per acre (t/acre), 0.113 t/acre, and 0.151 t/acre, respectively.

The agricultural salinity load was separated into three components: tail water, deep percolation, and canal seepage. Tail-water salinity loads ranged from 48.0 to 2,750 tons per year (t/yr) in the study area. The largest tail-water salinity load was in subbasin SF3, and the lowest salinity load from tail water was in subbasin R1. The remaining four agricultural subbasins—AL1, B1, CK1, and SF2—had tail-water loads of 285 t/yr, 180 t/yr, 333 t/yr, and 1,700 t/yr, respectively. The deep percolation component of the agricultural salinity load ranged from 3,300 t/yr in subbasin AL1 to 51,800 t/yr in subbasin SF2. Subbasins R1, B1, CK1, and SF3 had deep percolation salinity loads of 4,940 t/yr, 15,200 t/yr, 21,200 t/yr, and 23,600 t/yr, respectively. The

canal seepage component of the agricultural salinity load ranged from 1,100 t/yr in subbasin AL1 to 15,300 t/yr in subbasin CK1. Subbasins B1, R1, SF2, and SF3 had canal seepage salinity loads of 6,610 t/yr, 3,890 t/yr, 9,430 t/yr, and 12,100 t/yr, respectively.

Total salinity loads at each site were a combination of measured surface-water salinity loads and estimated groundwater salinity loads. Total salinity loads ranged from 27.9 ± 19.1 t/yr to $87,500 \pm 80,500$ t/yr. The four natural subbasins—BkKm, RCG1, RCG2, and SF1—had total salinity loads of 27.9 ± 19.1 t/yr, 371 ± 248 t/yr, $2,180 \pm 1,590$ t/yr, and $4,200 \pm 2,720$ t/yr, respectively. The agriculturally influenced sites had salinity loads that ranged from $7,580 \pm 6,900$ t/yr to $87,500 \pm 80,500$ t/yr. Salinity loads for subbasins AL1, B1, CK1, SF2, and SF3 were $7,580 \pm 6,900$ t/yr, $28,300 \pm 26,700$ t/yr, $48,700 \pm 36,100$ t/yr, $87,500 \pm 80,900$ t/yr, and $52,200 \pm 31,800$ t/yr, respectively.

It appears the pattern in the Smith Fork Creek region is for higher salinity loading to occur in agriculturally dominated subbasins. Subbasins with more irrigated land on Mancos Shale also tend to have higher salinity loads than subbasins that are not in the shale or have a mix of geology types. The natural subbasins generated little salinity load during the study period. The ephemeral stream characteristics of the natural subbasins indicate that agricultural influences are important in maintaining perennial streamflow in the agriculturally dominated subbasins.

Surface-water selenium loads were calculated for each subbasin and were considered the total selenium load because groundwater selenium loads were not estimated for the study period. It was determined that the mobilization mechanisms for selenium have multiple influences, but understanding and describing mobilization of selenium was outside the scope of this study. Three of the four natural subbasins had little to no selenium load based on the measured data and calculated selenium loads. Subbasins RCG1 and RCG2 had surface-water selenium loads of 0.106 ± 0.024 lb, and 0.00 lb, respectively. Subbasin BkKm did not have an estimated surface-water selenium load because of the lack of any water-quality samples during the study period. The subbasin designated by site CK1 had the highest selenium load with 135 ± 38.7 lb, and the next highest subbasins in decreasing order are B1, SF3, AL1, SF1, and R1 with selenium loads of 69.6 ± 28.4 lb, 56.5 ± 23.8 lb, 30.5 ± 16.6 lb, 26.8 ± 6.95 lb, and 15.6 ± 27.7 lb, respectively.

Acknowledgments

The authors of this report would like to thank the following individuals: Bethany Burton (U.S. Geological Survey) for her assistance in collecting data during the study, the Delta Soil Conservation District for supplying detailed canal mapping and flow information, Mike Baker (formally of the Bureau of Reclamation) for insight and knowledge during data collection, and Darwin Ockerman (U.S. Geological Survey) and Lindsay Ball (U.S. Geological Survey) for providing technical reviews.

References

- Allen, R.G., Pereira, L.S., Raes, Dirk, Smith, Martin, 1998, Crop evapotranspiration—Guidelines for computing crop water requirements: Food and Agriculture Organization of the United Nations, Irrigation and Drainage Paper, no. 56, 299 p.
- Andersen M.P., 2006, Heat as a ground water tracer: *Ground Water*, v. 43, no. 6, p. 951–968.
- Benson, M.A., and Dalrymple, Tate, 1967, General field and office procedures for indirect discharge measurements: U.S. Geological Survey Techniques of Water-Resources Investigations, book 3, chap. A1, 30 p.
- Blasch, K.J., Constantz, James, and Stonestrom, D.A., 2007, Thermal methods for investigating ground-water recharge, *in* Stonestrom, D.A., Constantz, James, Ferre, T.P.A., and Leake, S.A., eds., Ground-water recharge in the arid and semiarid southwestern United States: U.S. Geological Survey Professional Paper 1703, p. 353–376.
- Broner, Israel, and Schneekloth, J.P., 2003, Seasonal water needs and opportunities for limited irrigation for Colorado crops: Colorado State University Cooperative Extension, Crop series no. 4.718.
- Bureau of Reclamation, 1982, Hydrosalinity, app. B of Lower Gunnison Basin Unit—Feasibility report: Bureau of Reclamation, 86 p.
- Bureau of Reclamation, 2009a, CRBSCP, Lower Gunnison Basin Unit, Title II—Project details: Bureau of Reclamation, Colorado River Basin Salinity Control Program, accessed January 19, 2009, at http://www.usbr.gov/projects/Project.jsp?proj_Name=CRBSCP+-+Lower+Gunnison+Basin+Unit+-+Title+II.
- Bureau of Reclamation, 2009b, Western Colorado area office, water operations—Crawford Reservoir, Colorado: Bureau of Reclamation, Upper Colorado Region, accessed January 19, 2009, at <http://www.usbr.gov/uc/wcao/water/rsrvs/ds/crawford.html>.
- Butler, D.L., and Leib, K.J., 2002, Characterization of selenium in the Lower Gunnison River Basin, Colorado: U.S. Geological Survey Water-Resource Investigation Report 02–4151, 26 p. (Also available at <http://pubs.usgs.gov/wri/wri02-4151/>.)
- Chow, V.T., Maidment, D.R., and Mays, L.W., 1988, Applied hydrology: New York, McGraw-Hill, 572 p.
- Colorado's Decision Support System, 2005, GIS data—Division 4, Gunnison: Colorado Water Conservation Board and Colorado Division of Water Resources, accessed April 2014 at <http://cdss.state.co.us/GIS/Pages/Division4Gunnison.aspx>.
- Colorado Department of Public Health and Environment, 1983, Classifications and numeric standards for Gunnison and lower Dolores river basins: Colorado Department of Public Health and Environment, Water Quality Control Commission, Regulation no. 35. (Amended 2013.)
- Colorado State University, 2009, CoAgMet station summary access: Colorado State University, accessed September 2009 at http://ccc.atmos.colostate.edu/cgi-bin/stationsum_form.pl.
- Constantz, James, 2008, Analysis of temperature gradients to determine stream exchanges with ground water, *in* Rosenberry, D.O., and LaBaugh, J.W., eds., Field techniques for estimating water fluxes between surface water and ground water: U.S. Geological Survey Techniques and Methods, book 4, chap. D2, p. 115–128.
- Constantz, James, Stewart, A.E., Niswonger, Richard, and Sarma, Lisa, 2002, Analysis of temperature profiles for investigating stream losses beneath ephemeral channels: *Water Resources Research*, v. 38, no. 12, p. 1–13.
- Cox, M.H., Su, G.W., and Constantz, James, 2007, Heat, chloride, and specific conductance as ground water tracers near streams: *Ground Water*, v. 45, no. 2, p. 187–195.
- Daly, Christopher, Nielson, R.P., and Philips, D.L., 1994, A statistical-topographic model for mapping climatological precipitation over mountainous terrain: *Journal of Applied Meteorology*, v. 33, p. 140–158.
- Eddy-Miller, C.A., Wheeler, J.D., and Essaid, H.J., 2009, Characterization of interactions between surface water and near-surface groundwater along Fish Creek, Teton County, Wyoming, by using heat as a tracer: U.S. Geological Survey Scientific Investigations Report 2009–5160, 53 p.
- ESRI, 2010, ArcGIS—A complete integrated system: Redlands, Calif., Environmental Systems Research Institute (ESRI), <http://www.esri.com/software/arcgis/>.
- Essaid, H.I., Zamora, C.M., McCarthy, K.A., Vogel, J.R., and Wilson J.T., 2007, Using heat to characterize streambed water flux variability in four stream reaches: *Journal of Environmental Quality*, v. 36, p. 1–14.
- Fishman, M.J., and Friedman, L.C., 1989, Methods for determination of inorganic substances in water and fluvial sediments: U.S. Geological Survey Techniques of Water-Resources Investigations, book 5, chap. A1, 545 p.
- Freeze, R.A., and Cherry, J.A., 1979, Groundwater: Englewood, N.J., Prentice Hall, Inc., 604 p.
- Garrels, R.M., and Thompson, M.E., 1962, A chemical model for seawater at 25°C and one atmosphere total pressure: *American Journal of Science*, v. 260, p. 57–66.

- Hansen, W.R., 1987, The Black Canyon of the Gunnison, Colorado, *in* Beus, S.S., ed., Rocky Mountain section of the Geological Society of America. Centennial Field Guides, v. 2: Geological Society of America, Decade of North American Geology project, p. 321–327.
- Healy, R.W., and Ronan, A.D., 1996, Documentation of computer program VS2DH for simulation of energy transport in variably saturated porous media—Modification of the U.S. Geological Survey's computer program VS2DT: U.S. Geological Survey Water-Resources Investigations Report 96–4230, 40 p.
- Helsel, D.R., and Hirsch, R.M., 2002, Statistical methods in water resources: U.S. Geological Survey Techniques of Water-Resources Investigations, book 4, chap. A3, 510 p.
- Hem, J.D., 1989, Study and interpretation of the chemical characteristics of natural water (3d ed.): U.S. Geological Survey Water-Supply Paper 2254, 264 p.
- Howell, T.A., and Evett, S.R., 2004, The Penman-Monteith method: U.S. Department of Agriculture, Agricultural Research Service, 14 p.
- Jeton, A.E., Watkins, S.A., Lopez, T.J., and Huntington, Justin, 2005, Evaluation of precipitation estimates from PRISM for the 1961–90 and 1971–2000 data sets, Nevada: U.S. Geological Survey Scientific Investigations Report 2005–5291, 26 p.
- Lapalla, E.G., Healy, R.W., and Weeks, E.P., 1987, Documentation of computer program VS2D to solve the equations of fluid flow in variably saturated porous media: U.S. Geological Survey Water Resources Investigations Report 83–4099, 184 p.
- Laronne, J.B., 1977, Dissolution potential of superficial Mancos Shale and alluvium: Fort Collins, Colo., Colorado State University, Ph.D. dissertation, 128 p., 14 tables, 23 figures.
- Lemly, A.D., 2002, Selenium assessment in aquatic ecosystems—A guide for hazard evaluation and water-quality criteria: New York, Springer-Verlag, 161 p.
- Mayo, J.W., and Leib, K.J., 2012, Flow-adjusted trends in dissolved selenium load and concentration in the Gunnison and Colorado Rivers near Grand Junction, Colorado, water years 1986–2008: U.S. Geological Survey Scientific Investigations Report 2012–5088, 33 p.
- Meyer, P.D., Rockhold, M.L., and Gee, G.W., 1997, Uncertainty analyses of infiltration and subsurface flow and transport for SDMP sites: Prepared for U.S. Nuclear Regulatory Commission, Office of Nuclear Regulatory Research, Division of Regulatory Applications, NUREG/CR-6565, PNNL-11705, 38 p.
- Munsell Color, 1992, Munsell soil color charts: Newburg, N.Y., Macbeth Division of Kollmorgen Instruments Corporation, 10 p.
- New Mexico Climate Center, 2009, New Mexico crop information: New Mexico State University, New Mexico Climate Center, accessed September 18, 2009, at <http://hydrology1.nmsu.edu/nmcrops/>.
- Niswonger, R.G., and Prudic, D.E., 2003, Modeling heat as a tracer to estimate stream seepage and hydraulic conductivity, *in* Constantz, Jim, and Stonestrom, D.A., eds., Heat as a tool for studying the movement of ground water near streams: U.S. Geological Survey Circular 1260, p. 81–89.
- Pritt, J.Q., and Raese, J.W., 1992, Quality assurance/quality control manual: U.S. Geological Survey Open-File Report 92–0495, 33 p.
- Rantz, S.E., and others, 1982, Computation and discharge. Measurement and computation of streamflow, v. 2: U.S. Geological Survey Water-Supply Paper 2175, 346 p.
- Ronan, A.D., Prudic, D.E., Thodal, C.E., and Constantz, Jim, 1998, Field study and simulation of diurnal temperature effects on infiltration and variably saturated flow beneath an ephemeral stream: Water Resources Research, v. 34, no. 9, p. 2137–2153.
- Schaffrath, K.R., 2012, Surface-water salinity in the Gunnison River Basin, Colorado, water years 1989 through 2007: U.S. Geological Survey Scientific Investigations Report 2012–5128, 47 p.
- SonTek/YSI Inc., 2007, FlowTracker Handheld ADV technical manual: San Diego, Calif., SonTek/YSI Inc., 116 p.
- Stonestrom, D.A., and Constantz, Jim, 2003, Heat as a tool for studying the movement of ground water near streams: U.S. Geological Survey Circular 1260, 96 p.
- Taylor, J.R., 1997, An introduction to error analysis—The study of uncertainties in physical measurements (2d ed.): Sausalito, Calif., University Science Books, 327 p.
- Thomas, J.C., Leib, K.J., and Mayo, J.W., 2008, Analysis of dissolved selenium loading for selected sites in the Lower Gunnison River Basin, Colorado, 1978–2005: U.S. Geological Survey Scientific Investigations Report 2007–5287, 25 p.
- Topper, Ralf, Spray, K.L., Bellis, H.B., Hamilton, J.L., and Barkmann, P.E., 2003, Ground water atlas of Colorado: Colorado Geological Survey Special Publication 53, 209 p.
- Turnipseed, D.P., and Sauer, V.B., 2010, Discharge measurements at gaging stations: U.S. Geological Survey Techniques and Methods, book 3, chap. A8, 87 p. (Also available at <http://pubs.usgs.gov/tm/tm3-a8/>.)

- Tweto, Ogden, comp., 1979, Geologic map of Colorado: U.S. Geological Survey Map, scale 1:500,000.
- U.S. Census Bureau, 2009, 2010 Population finder: U.S. Census Bureau, accessed January 19, 2009, at <http://www.census.gov/popfinder/>.
- U.S. Geological Survey, 2009, 09134000 Minnesota Creek near Paonia, CO, in Water-Data Report 2009: U.S. Geological Survey, National Water Information System, accessed April 14, 2011, at <http://wdr.water.usgs.gov/wy2009/pdfs/09134000.2009.pdf>.
- U.S. Geological Survey, 2010, USGS 09152500 Gunnison River near Grand Junction, CO: U.S. Geological Survey National Water Information System, accessed January 13, 2010, at http://waterdata.usgs.gov/co/nwis/nwisman/?site_no=09152500.
- U.S. Geological Survey, 2011, Colorado StreamStats: U.S. Geological Survey, accessed April 18, 2011, at http://streamstatsags.cr.usgs.gov/co_ss/default.aspx.
- U.S. Geological Survey, [2013], Water quality samples for Colorado: U.S. Geological Survey, National Water Information System, accessed April 8, 2013, at http://waterdata.usgs.gov/co/nwis/dv/?referred_module=gw.
- U.S. Geological Survey, [variously dated], National field manual for the collection of water-quality data: U.S. Geological Survey Techniques of Water-Resources Investigations, book 9, chap. A1–A9.
- Wagner, R.J., Boulger, R.W., Jr., Oblinger, C.J., and Smith, B.A., 2006, Guidelines and procedures for continuous water-quality monitors—Station operation, record computation, and data reporting: U.S. Geological Survey Techniques and Methods 1–D3, 51 p., 8 attachments.
- Waskom, R., and Neibauer, M., 2006, Water conservation in and around the home: Colorado State University Extension, Fact Sheet 9.952, accessed January 29, 2010, at <http://www.ext.colostate.edu/pubs/consumer/09952.html>.
- Western Regional Climate Center, 2014, Climate of Colorado: Reno, Nev., Western Regional Climate Center, accessed April 29, 2014, at <http://www.wrcc.dri.edu/narratives/colorado/>.
- Zamora, Celia, 2008, Estimating water fluxes across the sediment-water interface in the Lower Merced River, California: U.S. Geological Survey Scientific Investigations Report 2007–5216, 47 p.

Appendixes

Appendix 1. Lithological Descriptions of Sediment Cores Collected from Various Drilled Well Holes at Sites Km and Kdb

[Munsell color classification codes are explained in Munsell Color (1992). For example, 2.5Y 4/2 gives the hue, value, and chroma of each color; where 2.5Y is the hue, 4 is the value, and 2 is the chroma. m, meter; n.a., not applicable; %, percent]

Depth, in meters	Lithology	Munsell color
Km_well1—lat 38°42'02.33"N., long 107°57'36.07"W. Measured depth of refusal—2.92 m		
0–0.18	No sample	n.a.
0.18–0.47	Clayey silt, soft, moist, organic, iron staining, interbedded roots, slightly calcareous throughout the interval	2.5Y 4/2
0.47–0.88	Silty sand, very fine, well sorted, well rounded, clay content 10–20%, moist, iron staining, interbedded roots, organic lens from 0.84 to 0.85 m (2.5Y 3/1), moderately calcareous throughout the interval	2.5Y 5/2
0.88–1.16	Clay, soft, moist, sticky, iron staining, interbedded shale toward the bottom, friable (5Y 5/2), some interbedded roots, moderately calcareous throughout the interval	5Y 5/3
1.16–1.5	Clayey silt, soft, interbedded silty shale, friable, slight moisture content, moderately calcareous throughout the interval	5Y 5/2
1.5–2.32	Shale, friable, harder than above, iron staining, slight moisture content, moderately calcareous throughout the interval	5Y 3/1
2.32–2.48	No sample	
2.48–2.92	Shale, friable, massive, hard, iron staining, yellowish red (5Y 5/6), slight moisture content, very calcareous throughout the interval	5Y 3/1
Km_well2—lat 38°42'02.28"N., long 107°57'36.07"W. Measured depth of refusal—0.61 m		
0–0.29	Clay, soft, sticky, moist, lenses of weathered shale, fissile, friable, (5Y 3/1), slightly calcareous throughout the interval	5Y 6/2
0.29–0.61	Shale, weathered, friable, fissile to massive, clay lenses, soft sticky, moist, moderately calcareous throughout the interval	5Y 4/1
Kdb_well1—lat 38°38'29.32"N., long 108°08'23.42"W. Measured depth of refusal—1.03 m		
0–0.18	No sample	n.a.
0.18–1.03	Clayey silt, soft, with sandstone lenses, fine, hard, iron staining, moist, interbedded roots, clay lens from 0.64 to 0.70 m, soft, (5Y 5/1), slightly calcareous throughout the interval	2.5Y 6/4
Kdb_well2—lat 38°38'29.41"N., long 108°08'23.10"W. Measured depth of refusal—0.85 m		
0–0.15	No sample	n.a.
0.15–0.51	Silty clay, soft, with sandstone lenses (2.5Y 6/4), soft, fine, friable, weathered, iron stained, slight moisture content, appearance of gypsum veins in the clay, moderately calcareous throughout the interval	2.5Y 4/1
0.51–0.65	Silty clay to weathered shale, fissile, some appearance of bedding, soft, slight moisture content	2.5Y 4/1
0.65–0.85	Sandstone, fine, weathered in spots, friable, silty clay lens at the bottom, soft, (2.5Y 4/1), slight moisture content in the clay	10YR 5/6

Appendix 2. Measured Canal Temperature and Specific Conductance Data in the Study Area

[°C, degree Celsius; µS/cm, microsiemen per centimeter; date given in DD-Month-YY; time given in HHMM on a 24-hr clock; --, no data available]

Canal name	Latitude	Longitude	Date	Time	Temperature, °C	Specific conductance, µS/cm
Cattleman's Ditch at J82 Road	38°33'14"	107°31'12"	16-Jul-08	1310	18.3	89
Cattleman's Ditch at J82 Road	38°33'14"	107°31'12"	2-Oct-08	1335	13.8	119
Clipper Ditch at Crawford	38°42'15"	107°36'48"	12-Mar-08	--	5.1	930
Clipper Ditch at Crawford	38°42'15"	107°36'48"	12-May-08	1550	10	155
Clipper Ditch at Crawford	38°42'15"	107°36'48"	16-Jul-08	1200	19.1	724
Clipper Ditch at Crawford	38°42'15"	107°36'48"	2-Oct-08	1235	11.1	775
Clipper Ditch at Crawford	38°42'15"	107°36'48"	4-Dec-08	1220	3.7	415
Cottonwood Canal at F Road	38°43'35"	107°33'59"	19-May-08	1500	12.3	150
Cottonwood Canal at F Road	38°43'35"	107°33'59"	16-Jul-08	1145	15.1	174
Cottonwood Canal at F Road	38°43'35"	107°33'59"	2-Oct-08	1220	13.2	216
Cottonwood Canal at F Road	38°43'35"	107°33'59"	4-Dec-08	1130	1.2	150
Crawford Reservoir Syphon	38°42'02"	107°37'11"	16-Jul-08	1205	8.6	820
Crawford Reservoir Syphon	38°42'02"	107°37'11"	2-Oct-08	1240	16.5	999
Crawford Road Reservoir Syphon	38°42'02"	107°37'11"	4-Dec-08	1225	5.8	719
Fruitland Mesa Ditch at Hwy 92	38°32'56"	107°32'30"	16-Jul-08	1245	24.1	441
Fruitland Mesa Ditch at Hwy 92	38°32'56"	107°32'30"	2-Oct-08	1325	15.4	443
Gould Canal at Black Canyon Road	38°39'19"	107°39'08"	19-May-08	1405	12.6	257
Gould Canal at Black Canyon Road	38°39'19"	107°39'08"	16-Jul-08	1400	17.1	277
Grand View Canal	38°41'57"	107°37'24"	7-Mar-08	1203	3.1	1,160
Grand View Canal	38°41'57"	107°37'24"	12-May-08	1630	9.6	283
Grand View Canal	38°41'57"	107°37'24"	16-Jul-08	1210	10.0	840
Grand View Canal	38°41'57"	107°37'24"	2-Oct-08	1245	16.7	1,012
Grand View Canal	38°41'57"	107°37'24"	4-Dec-08	1230	5.5	729
Grand View Canal near Alum Gulch	38°43'16"	107°43'34"	7-Mar-08	1520	5.6	1,520
Grand View Canal near Alum Gulch	38°43'16"	107°43'34"	16-Jul-08	1520	17.6	817
Grand View Canal near Alum Gulch	38°43'16"	107°43'34"	2-Oct-08	1450	18.1	973
Grand View Canal near Alum Gulch	38°43'16"	107°43'34"	4-Dec-08	1300	3.9	681
Minnesota Ditch at 4050 Road	38°50'25"	107°36'08"	16-Jul-08	1115	17.1	606
Minnesota Ditch at 4050 Road	38°50'25"	107°36'08"	2-Oct-08	1155	12.6	741
Minnesota Ditch at 4050 Road	38°50'25"	107°36'08"	4-Dec-08	1110	3.4	1,061
Minnesota Ditch at N25 Road	38°50'45"	107°35'28"	16-Jul-08	1055	13.4	341
Minnesota Ditch at N25 Road	38°50'45"	107°35'28"	2-Oct-08	1145	12.1	803
Minnesota Ditch at N25 Road	38°50'45"	107°35'28"	4-Dec-08	1106	2.4	530
Stewart Ditch at 4050 Road	38°51'02"	107°36'16"	16-Jul-08	1105	15.9	220
Stewart Ditch at 4050 Road	38°51'02"	107°36'16"	2-Oct-08	1150	12.6	282
Stewart Ditch at 4050 Road	38°51'02"	107°36'16"	4-Dec-08	1105	3.7	1,180
Minnesota Ditch at N25 Road	38°50'45"	107°35'28"	16-Jul-08	1055	13.4	341
Minnesota Ditch at N25 Road	38°50'45"	107°35'28"	2-Oct-08	1145	12.1	803
Minnesota Ditch at N25 Road	38°50'45"	107°35'28"	4-Dec-08	1106	2.4	530

Publishing support provided by:
Denver Publishing Service Center, Denver, Colorado

For more information concerning this publication, contact:
Director, USGS Colorado Water Science Center
Box 25046, Mail Stop 415
Denver, CO 80225
(303) 236-4882

Or visit the Colorado Water Science Center Web site at:
<http://co.water.usgs.gov/>

This publication is available online at:
<http://dx.doi.org/10.3133/sir20145101>

